Available online at www.sciencedirect.com

SCIENCE DIRECT

Developmental Biology 278 (2005) 396–414

DEVELOPMENTAL BIOLOGY

www.elsevier.com/locate/ydbio

The role of *Fgf*10 signaling in branching morphogenesis and gene expression of the rat prostate gland: lobe-specific suppression by neonatal estrogens

Liwei Huang, Yongbing Pu, Shumyle Alam, Lynn Birch, Gail S. Prins*

Department of Urology, University of Illinois at Chicago, 820 Wood Street, M/C 955 Chicago, IL 60612, USA

Received for publication 23 July 2004, revised 10 November 2004, accepted 12 November 2004
Available online 15 December 2004

Abstract

Brief exposure of rats to high-dose estrogen during the neonatal period interrupts prostate development in a lobe-specific manner and predisposes the gland to dysplasia with aging, a phenomenon referred to as developmental estrogenization. Our previous studies have revealed that these effects are initiated through altered steroid receptor expression; however, the immediate downstream targets remain unclear. We have recently shown that developmental expression of *Shh-ptc-gli* is downregulated in the dorsolateral prostate following estrogenization, and this is responsible, in part, for branching deficits observed in that prostatic region specifically. In the present study, we examine the role of *Fgf*10 signaling during rat prostate development and as a mediator of the developmental estrogenized phenotype. *Fgf*10 and *Fgf*R2*iii*b localize to the distal signaling center of elongating and branching ducts in separate prostate lobes where they regulate the expression of multiple morphoregulatory genes including *Shh*, *ptc*, *Bmp*7, *Bmp*4, *Hox*b13, and *Nkx*3.1. Ventral and lateral lobe organ cultures and mesenchyme-free ductal cultures demonstrate a direct role for *Fgf*10/*Fgf*R2*iii*b in ductal elongation, branching, epithelial proliferation, and differentiation. Based on these findings, a model is proposed depicting the localized expression and feedback loops between several morphoregulatory factors in the developing prostate that contribute to tightly regulated branching morphogenesis. Similar to *Shh-ptc-gli*, neonatal estrogen exposure downregulates *Fgf*10, *Fgf*R2*iii*b, and *Bmp*7 expression in the dorsolateral prostate while ventral lobe expression of these genes is unaffected. Lateral prostate organ culture experiments demonstrate that growth and branching inhibition as well as *Fgf*10/*Fgf*R2*iii*b suppression are mediated directly at the prostatic level. Furthermore, exogenous *Fgf*10 fully rescues the growth and branching deficits due to estrogen exposure. Together, these studies demonstrate that alterations in *Fgf*10 signaling are a proximate cause of *Shh-ptc-gli* and *Bmp*7 downregulation that together result in branching inhibition of the dorsolateral prostate following neonatal estrogen exposure.

Keywords: *Fgf*10; *Fgf*R2*iii*b; *Bmp*4; *Bmp*7; Sonic hedgehog; Patched; Prostate; Estrogen; Estradiol

Introduction

Development of the rat prostate gland is initiated late in fetal life (*f*18.5) when epithelial buds from the urogenital sinus (UGS) penetrate into the surrounding urogenital mesenchyme in ventral, lateral, and dorsal directions giving rise to the separate ventral (VP), lateral (LP) and dorsal lobes (DP), respectively. At the time of birth, the rat prostate is rudimentary, consisting of several solid, unbranched epithelial cords, and branching morphogenesis followed by cytologic and functional differentiation occurs during the immediate postnatal period (Hayashi et al., 1991). While androgens are both necessary and sufficient for prostate morphogenesis, the direct targets of androgen action during this developmental process are not well understood. In addition to androgens, it is recognized that other hormones influence prostate development including prolactin (Robertson et al., 2003), growth hormone (Ruan et al., 1999), retinoids (Aboseif et al., 1997; Seo et al., 1997), and

* Corresponding author. Fax: +1 312 996 1291.
E-mail address: gprins@uic.edu (G.S. Prins).

0012-1606/$ - see front matter © 2004 Elsevier Inc. All rights reserved.
doi:10.1016/j.ydbio.2004.11.020

estrogens (Huang et al., 2004; Price, 1936). Importantly, alterations in the balance of these hormones lead to distinctive changes in prostate development and function. Work from our laboratory has shown that brief exposure of the rat to estrogens during the critical neonatal period alters prostate branching morphogenesis and cellular differentiation in a dose-dependent manner (Prins and Birch, 1995; Putz et al., 2001). If estrogenic exposures are high, these disturbances lead to permanent and lobe-specific imprints of the prostate, a process referred to as developmental estrogenization. While all lobes present with hypoplasia, epithelial differentiation defects and altered secretory function are most pronounced in the VP whereas the DP and LP exhibit marked branching deficits (Chang et al., 1999; Habermann et al., 2001; Prins, 1992; Prins et al., 1993; Pu et al., 2004). Importantly, developmental estrogenization is associated with severe prostatic lesions with aging including epithelial hyperplasia, prostatic intraepithelial neoplasia (PIN), adenomas, and chronic inflammation (Gilleran et al., 2003; Prins, 1997; Putz and Prins, 2002). Thus, neonatal estrogenization of the rat prostate serves as a useful model for evaluating the role of endogenous and exogenous estrogens as a predisposing factor for prostatic disease later in life.

A fundamental understanding of the estrogenization phenomenon requires knowledge of the immediate cellular and molecular changes induced by estrogens that, in turn, alter the course of prostatic development long after hormone withdrawal. Toward that end, our studies have revealed that high-dose estrogens markedly alter the expression of key steroid receptors within the developing prostate (for review, see Prins et al., 2001b). Androgen receptors (ARs) are permanently downregulated (Prins, 1992; Prins and Birch, 1995; Woodham et al., 2003) while estrogen receptor α (ERα), progesterone receptor (PR), and retinoid receptors RAR/RXR are upregulated in a cell-specific and lobe-specific manner (Prins and Birch, 1997; Prins et al., 2001a,b, 2002; Pu et al., 2003; Sabharwal et al., 2000). The net result of these alterations is that prostate development is no longer under predominant androgen regulation but is rather driven by alternate steroids, principally estrogens and retinoids via their cognate receptors. We hypothesized that the overall effect of these changes is the programming, and organizational signals that normally dictate prostate development during discrete temporal windows are permanently and irretrievably altered.

Several genes that determine and regulate prostate development include common and tissue-specific transcription factors (e.g., *Nkx*3.1, *Fox*A1, *Hox*a13, *Hox*b13, and *Hox*d13) and secreted morphogens that establish reciprocal cross-talk between stromal and epithelial cells via their cognate receptors (e.g., *Shh*, *Fgf*7, *Fgf*10, *Bmp*7, *Bmp*4, *Tgf*β, and activins) (for review, see Huang et al., 2004). In the prostate, expression of these transcription and growth factors varies along the length of the elongating ducts giving rise to a unique distal signaling center that directs ductal outgrowth and branching (Pu et al., 2004). Our recent studies on *Shh-ptc-gli* expression in the developing rat prostate revealed distal tip localization of this signaling pathway with evidence for its direct involvement in branching morphogenesis (Pu et al., 2004). Importantly, *Shh* was shown to downregulate *Fgf*10 and upregulate *Bmp*4 expression in the developing prostate, suggesting that its effects on ductal branching may involve cross-talk with growth factor networks. In the estrogenized prostate, *Shh-ptc-gli* expression was rapidly downregulated in the LP and DP but not in the VP that directly correlated with branching inhibition in the DLP specifically. However, since prostatic estrogenization is mediated through mesenchymal ERα (Prins et al., 2001a,b), epithelial *Shh* downregulation is likely mediated through mesenchymal paracrine factors. In this study, we test the hypothesis that *Fgf*10 signaling may be directly altered by neonatal estrogen exposure and that its downstream actions may mediate specific aspects of the estrogenized phenotype.

*Fgf*10 is expressed by mesenchymal cells and has been previously identified as a critical morphogen involved in branching morphogenesis of a number of organs including the prostate gland (Bellusci et al., 1997; Cardoso, 2001; Donjacour et al., 2003; Hoffman et al., 2002; Thomson and Cunha, 1999; Weaver et al., 2000). *Fgf*10 is a member of the fibroblast growth factor (*Fgf*) family of secreted morphogens that consist of 23 known members (Ornitz and Itoh, 2001; Raman et al., 2003). *Fgf*s have a high affinity for heparin and glycosaminoglycans (GAGs), which position them for interaction with membrane-associated tyrosine kinase *Fgf* receptors (*Fgf*R) on target cells (Uematsu et al., 2000). The splice variant of *Fgf*R2, *Fgf*R2*iii*b, is the specific receptor for *Fgf*10 and is expressed by epithelial cells, thus establishing a stromal–epithelial loop (Finch et al., 1995). In the prostate gland, as in the lungs and other branched structures, *Fgf*10 expression is spatially restricted to the distal aspects of the glands where it is believed to function as a chemoattractant for elongating ducts and an inducer of ductal branching through stimulation of epithelial cell proliferation (Donjacour et al., 2003; Lu et al., 1999; Thomson and Cunha, 1999). In other systems, *Fgf*10 actions are also mediated, in part, through regulation of multiple signaling cascades, including *Shh* (Cardoso, 2001; Chuang and McMahon, 2003; Haraguchi et al., 2000; Revest et al., 2001). Downstream gene targets of *Fgf*10 action in the prostate gland have not been identified.

Regulation of *Fgf*10 signaling in developing organs is not well understood at present. It is currently hypothesized that localized regulation of *Fgf*10 expression at discreet foci may be involved in tightly controlling branching at precise sites (Chuang and McMahon, 2003; Weaver et al., 2000). We have recently shown that *Shh* downregulates *Fgf*10 expression in the prostate gland (Pu et al., 2004) and proposed that focal expression domains of *Shh* and *Fgf*10 play a role in dichotomous branching (Pu et al., 2004). *Tgf*β1 has recently been shown to downregulate prostatic *Fgf*10 expression

(Tomlinson et al., 2004), which is highly relevant since mesenchymal *Tgf*β1 plays an important role during prostate development and neonatal estrogens alter its levels and localization (Chang et al., 1999). The issue of whether androgens play a major role in regulating *Fgf*10 expression in the prostate gland is presently unresolved. While dihydrotestosterone markedly induced *Fgf*10 expression in cultured prostate stromal cells (Lu et al., 1999), stimulation of *Fgf*10 expression by testosterone in rat VP organ culture was modest, suggesting that androgens may not be a principal *Fgf*10 regulator in vivo (Thomson and Cunha, 1999). Nonetheless, it is possible that a shift from normal androgen-dominated morphogenesis to developmental regulation by alternate steroids including retinoids, as occurs after neonatal estrogen exposure, may result in altered regulation of *Fgf*10 expression. It is noteworthy that retinoic acid selectively regulates *Fgf*10 expression in the gut (Desai et al., 2004) and that loss of *Fgf*10 inhibition by retinoic acid in the lungs is required for distal lung formation (Cardoso, 2001). Finally, while *Fgf*R2*iii*b is known to be expressed in prostatic epithelial cells, its spatiotemporal expression pattern and its regulation by steroids have not been previously examined.

The present study was designed to fully characterize the staged, spatiotemporal expression of *Fgf*10 and *Fgf*R2*iii*b in separate developing rat prostate lobes and to further define the role of this morphoregulatory pathway in prostate growth, ductal branching, and epithelial differentiation. To elucidate the mechanisms of these effects, we examined a number of candidate genes as potential downstream targets for *Fgf*10 action in the prostate gland. We then sought to determine whether *Fgf*10 and *Fgf*R2*iii*b expression are regulated by estrogens in the developing prostate gland and whether a disturbance in this signaling pathway may directly mediate neonatal estrogenization. Our findings demonstrate that *Fgf*10 and *Fgf*R2*iii*b are localized to the distal signaling center of elongating and branching prostatic ducts and that this signaling pathway regulates several developmental genes including *Shh*, *Bmp*4, *Bmp*7, *Nkx*3.1, and *Hox*b13. Neonatal estrogens directly suppress *Fgf*10 and *Fgf*R2*iii*b expression both in vivo and in vitro in the LP and DP but not the VP. Furthermore, organ culture studies show that *Fgf*10 replacement can rescue LP growth and branching inhibition as a result of estradiol administration. Taken together, these findings support the hypothesis that *Fgf*10 signaling plays a critical role, both directly and indirectly through alterations in other morphoregulatory genes, in mediating the estrogenized phenotype in the dorsolateral prostate.

Materials and methods

Animals

All rats were handled in accordance with the principles and procedures of the *Guiding Principles for the Care and Use of Animal Research* and the experiments were approved by the Institutional Animal Care Committee. Timed pregnant female Sprague–Dawley rats were purchased from Zivic-Miller (Pittsburgh, PA), housed individually in a temperature (21°C)- and light (14 h light/10 h dark)-controlled room, and fed standard Purina rat chow (Ralston-Purina, St. Louis, MO) ad libitum. The day of birth was designated as day 0. All males from a single mother were assigned to one of two groups and treated on postnatal days (pnd) 0, 3, and 5 with subcutaneous injections of either 25 μg 17β-estradiol-3-benzoate (Sigma-Aldrich Chemical Co., St. Louis, MO) in 25 μl of peanut oil (*Arachis* sp.) or with oil alone as controls. Pups were sacrificed by decapitation on pnd 1, 3, 6, 10, 15, 30, or 90 and the UGS–prostate complexes were dissected for subsequent analysis. Thus pups killed on pnd 1 and 3 were exposed to a single dose of estradiol on day 0 while offsprings killed on pnd 6 and later were exposed three times to estradiol.

In vitro estrogenic exposure

Since the in vivo estrogenic effects on *Fgf*10 and *Fgf*R2*iii*b expression were concentrated in the LP, in vitro experiments were performed with this lobe to determine if the effect was mediated directly at the prostatic level. LPs were isolated from pups ($n = 10$) on pnd 0 and cultured for 6 days as previously described (Pu et al., 2004) in basal organ culture medium (BOCM) in the absence or presence of 20 μM estradiol (Sigma-Aldrich) with medium changed every 48 h. To limit experimental variability, contralateral lobes from a single animal were paired and cultured with or without estradiol. BOCM consisted of DMEM/F-12 (Invitrogen, Carlsbad, CA), 10^{-8} M testosterone (Sigma-Aldrich), 50 μg/ml gentamycin, and 1× insulin-transferrin-selenium (Invitrogen). To monitor growth, daily photographs were captured with a Burle video camera and Snappy ver. 3.0 software and 2D area was calculated using Zeiss Image ver. 3.0 software (Carl Zeiss, Inc., Thornwood, NY). After 6 days, the urethral compartment was removed and the prostatic compartment was used for RNA isolation and real-time RT-PCR. In a separate series, the entire UGS–prostatic complex ($n = 6$) was removed on pnd 0, cultured as above with and without estradiol for 48 h, and fixed for subsequent whole mount in situ hybridization.

To determine if the estrogenic effect could be reversed with exogenous *Fgf*10, LPs were isolated from pups ($n = 12$) on pnd 0 and cultured as described above in (1) BOCM + 0.5 μg/ml BSA, (2) BOCM + BSA + 20 μM estradiol, or (3) BOCM + estradiol + 0.5 μg/ml *Fgf*10 (R&D Systems, Minneapolis, MN). Heparin (2.5 μg/ml; Sigma-Aldrich) was added to each culture group for the first 48 h of culture to aid in *Fgf*10 association with the extracellular matrix (ECM). To allow direct comparisons, groups 2 and 3 used the two LPs from a single animal. Daily photographs were taken to monitor growth and determine 2D area. On

the sixth day, the LPs were fixed and embedded in paraffin for subsequent immunocytochemistry.

Prostate organ culture and mesenchyme-free ductal culture with Fgf10

To examine the effects of *Fgf*10 on normal prostate development, rudimentary VPs and LPs (n = 6) were removed on pnd 0 and paired lobes from a single pup were cultured for 6 days in the presence or absence of 0.5 μg/ml *Fgf*10 in BOCM with 2.5 μg/ml heparin for the first 48 h of culture. Daily photographs were taken everyday to monitor growth. On day 6, tissues were fixed and embedded in paraffin for subsequent immunocytochemistry. In a separate set of similarly treated LPs (n = 7), the cultures were pulsed on day 6 with 10 μM BrdU (Sigma-Aldrich) for 2.5 h, washed in PBS for 30 min, fixed overnight in methacarn, and embedded in paraffin. To determine whether testosterone affects *Fgf*10 and *Fgf*R2*iii*b expression, an additional set (n = 8) of LPs and VPs was removed on pnd 0 and contralateral lobes were cultured for 20 h in BOCM with or without 10^{-8} M testosterone. The individual lobes were homogenized and total RNA isolated for real-time RT-PCR to quantitate *Fgf*10 and *Fgf*R2*iii*b mRNA levels.

To examine the effects of *Fgf*10 on gene expression in the normal developing prostate, rudimentary VPs (n = 8) were removed on pnd 0 and paired lobes from a single pup were cultured with or without exogenous *Fgf*10 in BOCM minus testosterone. After 24 h, tissues were homogenized and total RNA isolated for subsequent real-time RT-PCR. In a separate series, the entire UGS–prostatic complex (n = 3) was removed on pnd 0, cultured as above for 24 h, and fixed for subsequent whole mount in situ hybridization.

Mesenchyme-free prostatic ductal cultures were performed to examine the role of *Fgf*10 in ductal growth and branching. VPs were removed on pnd 0 and digested with 0.05% collagenase (Sigma-Aldrich) in phenol-free Hank's salt solution (Sigma-Aldrich) containing 1% fetal bovine serum (FBS; Sigma-Aldrich) for 45 min at 37°C, washed twice in Hank's with 10% FBS, and the epithelium and mesenchyme were separated with tungsten needles. The epithelial ducts were further digested with 1.6 U/ml dispase (BD Biosciences, San Jose, CA) for 10 min at 37°C and washed twice in Hank's with 10% FBS. The distal epithelial rudiments were embedded in growth factor reduced Matrigel (BD Biosciences) and cultured for 44 h in culture medium with 10^{-8} M testosterone or 0.5 μg/ml *Fgf*10. To examine the *Fgf*10 signaling pathway, *Fgf*10-treated ducts were cultured in the presence of the *Mek* inhibitor U0126 (20 μM; Calbiochem, San Diego, CA). Mesenchyme-free experiments were repeated 4–8 times.

Whole mount in situ hybridization (wmISH)

The UGS–prostatic complexes were fixed in 4% paraformaldehyde, dehydrated, and digested with proteinase K. Following prehybridization, tissues were hybridized overnight at 60°C with 0.5–0.6 μg/ml digoxigenin-labeled RNA probe, washed at high and low stringency, incubated overnight at 4°C in anti-digoxygenin alkaline phosphatase-conjugated antiserum (Roche, Indianapolis, IN), and color reacted with NBT and BCIP (Roche). To allow for temporal and treatment comparisons, pnd 1, 3, and 6 prostatic complexes from in vivo control and estrogenized rats were processed together and direct comparisons were made within each run. A minimum of four separate wmISH assays were performed for *Fgf*10 and *Fgf*R2*iii*b from in vivo experiments. The prostates were photographed with a Carl Zeiss AxioCam color digital camera using AxioVision ver. 2.0.5 software. To identify cellular localization of gene expression, wmISH-stained tissues were cross-sectioned at 10 μm.

The rat *Fgf*10, *Fgf*R2*iii*b, and *Bmp*7 templates were prepared by TA cloning 498-, 570-, and 344-bp PCR fragments, respectively, into PCR II vectors. The plasmids were sequenced to confirm PCR precision and orientation. The plasmids were linearized with the following restriction enzymes: *Fgf*10 with *Eco*RV (antisense) and *Spe*I (sense), *Fgf*R2*iii*b with *Hin*dIII (antisense) and *Xho*I (sense), and *Bmp*7 with *Spe*I (antisense) and *Not*I (sense). Digoxigenin-labeled RNA probes were prepared by in vitro transcription using appropriate RNA polymerases (DIG RNA labeling kit, Roche).

Immunocytochemistry (ICC)

*Fgf*10, *Fgf*R2*iii*b, and p63, a basal cell marker, were localized by immunocytochemistry as described (Prins et al., 1991). For *Fgf*10 and *Fgf*R2*iii*b, tissues were frozen in Tissue-Tek O.C.T. compound (Sakura Finetek, USA, Inc., Torrence, CA) and frozen sections were fixed in 2% paraformaldehyde. For p63, paraffin-embedded sections were heat treated in a Deloaker pressure cooker (Biocare Medical, Walnut Creek, CA) in 0.1 M citrate buffer, pH 6.0. Sections were next blocked with 2% serum and incubated overnight at 4°C with goat anti-*Fgf*10 antibody (1:100, sc-7375; Santa Cruz Biotechnology, Inc., Santa Cruz, CA), goat anti-*Fgf*R2*iii*b antibody (1:200, sc-122; Santa Cruz), or rabbit anti-p63 antibody (1:500, sc-8343; Santa Cruz). The sections were reacted with biotinylated anti-IgG (Vector Laboratories, Inc., Burlingame, CA) and detected with avidin–biotin peroxidase (ABC-Elite, Vector Laboratories) using diaminobenzidine tetrachloride (DAB) as chromagen. For controls, normal goat or rabbit IgG was substituted for primary antibody. The sections were counterstained with Gill's #3 hematoxylin (1:4).

ICC was used to localize BrdU-labeled cells from organ culture studies according to the method of McGinley et al. (2000). Paraffin blocks were sectioned along the longitudinal axis of the gland, sections (5 μm) were hydrolyzed in 2 N HCl for 90 min, and endogenous peroxide was blocked with 3% H_2O_2. Sections were incubated with

mouse anti-BrdU (Roche), biotinylated horse anti-mouse antibody (Vector Laboratories), and detected with avidin–biotin peroxidase using DAB as a chromagen followed by counterstain with Harris hematoxylin. Labeled epithelial cells in the proximal and centro-distal ducts were counted using Zeiss Image ver. 3.0 software and a proliferation index was determined by calculating the number of positively labeled epithelial cells per square micrometer multiplied by 1000. Ducts in the glandular area closest to the urethra that had not yet branched were considered proximal ducts. The remainder of the gland was considered centro-distal ducts.

Real-time RT-PCR

Two procedures were used for RNA extraction and reverse transcription (RT) depending upon tissue volume. A standard assay for pnd 6–90 VP involved RNA extraction with Trizol (Invitrogen), DNase I digestion (Roche), and RT with AMV at 42°C for 60 min using the RT System (Promega, Madison, WI). For smaller tissues (pnd 1–6 VP, pnd 3–10 LP and DP, and cultured prostate lobes), a RNeasy Kit (Qiagen, Valencia, CA) was used for RNA extraction, On-Column DNase I digestion, and RT with MMLV at 37°C for 60 min using First Strand cDNA Synthesis Kit (Fermentas Inc., Hanover, MD). Random primers were used for reverse transcription.

Real-time PCR was performed in duplex with Platinum qPCR Supermixture-UDG (Invitrogen) using an iCycler (Bio-Rad, Hercules, CA). Reaction conditions were optimized for each gene and the cycle conditions were 95°C for 3 min and 40 cycles of 95°C for 15 s and 60°C for 30 s. The exon-spanning primers and dual-labeled probes are listed in Table 1. For dual-labeled probes, 5′-reporters were FAM for *Fgf*10, *Fgf*R2*iii*b, *Shh*, *Bmp*4 and *Hox*b13; Hex for *ptc* and *Rpl*19; and the 3′-reporter was labeled with black hole quencher. SYBR green assay was performed for *Bmp*7 and *Nkx*3.1, and melting curve analysis confirmed the product specificity. Plasmids containing each DNA sequence (*Fgf*10, *Fgf*R2*iii*b, *Shh*, *ptc*1, *Bmp*4, *Hox*b13, and *Rpl*19) were cloned with TOPO TA cloning kit (Invitrogen) and used for standard curves in each reaction to directly quantitate target DNA levels. Ribosomal Protein L19 (*Rpl*19) was quantitated and served as an internal reference for normalization. Direct comparisons of *Rpl*19 per unit total RNA revealed no effect of estrogen treatment in developing prostates. Optical data obtained by real-time PCR were analyzed with the manufacturer's software (iCycle Optical System Interface ver. 3.0). Each assay was repeated 3–10 times using different tissues.

Statistical analysis

Tissue 2D area, BrdU labeling, and RT-PCR results were analyzed by two-tailed Student's *t* test (2 group comparisons) or, for multiple groups, analysis of variance followed by Bonferroni's post hoc tests (Instat ver. 3.01, GraphPad Software, Inc., San Diego, CA).

Table 1
Primers and Taqman probes used for RT-PCR

Gene	Sequence	GenBank GI #	Amplicon size (bp)
Fgf10			
Forward primer	cgtcaaagccattaacagca	6978836	107
Reverse primer	cctctatcctctctttcagtttacagt		
Probe	tgagccatagagtttccccttcttgttc		
FgfR2iiib			
Forward primer	gacgtagaatttgtctgcaagg	11139011	81
Reverse primer	actgccgttctttttccaca		
Probe	atagtgatgcccagccccatatcca		
Shh			
Forward primer	caattacaaccccgacatca	8394266	142
Reverse primer	agtcactcgaagcttcactcc		
Probe	ctctgagtcatcagccggtctgctc		
ptc1			
Forward primer	tcacagagacagggtacatgg	4092049	104
Reverse primer	cccggactgtagctttgc		
Probe	ccttcccagaagcagtccaaaggtg		
Bmp4			
Forward primer	gattggctcccaagaatcat	6978570	114
Reverse primer	cctagcaggacttggcataa		
Probe	cgaccatcagcattcggttaccag		
Bmp7			
Forward primer	agtgtgccttccctctgaac	3337107	99
Reverse primer	agggcttgggtacggtgt		
Nkx3.1			
Forward primer	ccgagtctgatgcacatttt	2105349	95
Reverse primer	ctgtggctgcttggtgac		
Hoxb13			
Forward primer	gatgtgttgccaaggtgaac	6680246	83
Reverse primer	gaggagggtgctggacac		
Probe	aaagcagcgtttgcagagcc		
Rpl19			
Forward primer	ggaagcctgtgactgtccat	14389296	101
Reverse primer	ggcagtacccttcctcttcc		
Probe	aagggcaggcatatgggcat		

Designed using the following websites: http://www.bioinfo.rpi.edu/applications/mfold/old/dna/, http://frodo.wi.mit.edu/cgi-bin/primer3/primer3_www.cgi.

Results

Fgf10 and FgfR2iiib in the developing rat prostate

Whole mount ISH and real-time RT-PCR were used to examine the spatial and temporal expression patterns of *Fgf*10 and *Fgf*R2*iii*b in the developing rat prostate lobes during the active period of branching morphogenesis. While the spatial expression patterns were similar between

the three lobes, the temporal expression pattern of these genes in the DP and LP was shifted 2–3 days later than the more rapidly developing VP. On pnd 1, the earliest time point examined in this study, the unbranched DP and LP epithelial buds were beginning to penetrate the prostatic mesenchyme while the VP ducts had elongated into the mesenchymal pad and dichotomous branching had begun. At this time, there was broad expression of *Fgf*10 mRNA in the DP and LP distal mesenchyme while the penetrating epithelial buds were negative, providing a punched-hole appearance to the ducts (Fig. 1A). In the VP, *Fgf*10 expression was also greatest in the distal mesenchyme and had begun to localize most intensely to the condensed mesenchyme surrounding the distal aspects of the elongating and branching ducts. By pnd 3, this localization pattern was also evident in DP and LP ducts (Fig. 1B). By pnd 6, the intensity of the *Fgf*10 signal had declined and was primarily localized to the periductal mesenchyme in all lobes (Fig. 1C). Microdissection of a VP sublobe (Fig. 1G) and distal tip (Fig. 1I) from a pnd 6 prostate permitted clear demonstration of the distal concentration of this morphogen in the condensed mesenchyme immediately adjacent to the elongating and branching epithelial ducts. Quantitation of absolute levels of *Fgf*10 mRNA by real-time RT-PCR over time confirmed that the highest expression in the VP was at pnd 1 and levels declined thereafter to a nadir at day 30 where they remained through adulthood (Fig. 2A, solid circles). DP and LP levels were quantified during the early developmental periods and total prostatic levels held steady between pnd 3 and 10 in those regions. Testosterone exposure for 18 h did not influence *Fgf*10 transcript levels in either the VP or LP during the developmental period (Fig. 2B).

As a counterpart to its secreted ligand, *Fgf*R2*iii*b expression was confined to epithelial cells in the distal regions of the elongating and branching ducts in all prostate lobes between pnd 1 and 6 (Figs. 1D–F). Microdissection of a pnd 6 VP sublobe (Fig. 1H) revealed lack of proximal duct *Fgf*R2*iii*b mRNA and an increasing expression gradient along the central–distal axis with the highest signal at the distal tips. Further, a dissected VP distal tip (Fig. 1J) and cross-sectional analysis (data not shown) confirmed the strict epithelial localization of this receptor. Quantitation of *Fgf*R2*iii*b mRNA levels in the separate lobes by real-time RT-PCR revealed that VP expression levels were highest at pnd 3, and declined thereafter to a nadir at day 30 where they remained (Fig. 2). Similarly, DP and LP total *Fgf*R2*iii*b expression declined significantly by pnd 10 as compared to pnd 6. Exposure to testosterone for 18 h did not affect *Fgf*R2*iii*b mRNA levels in either the VP or LP during the developmental period (Fig. 2B).

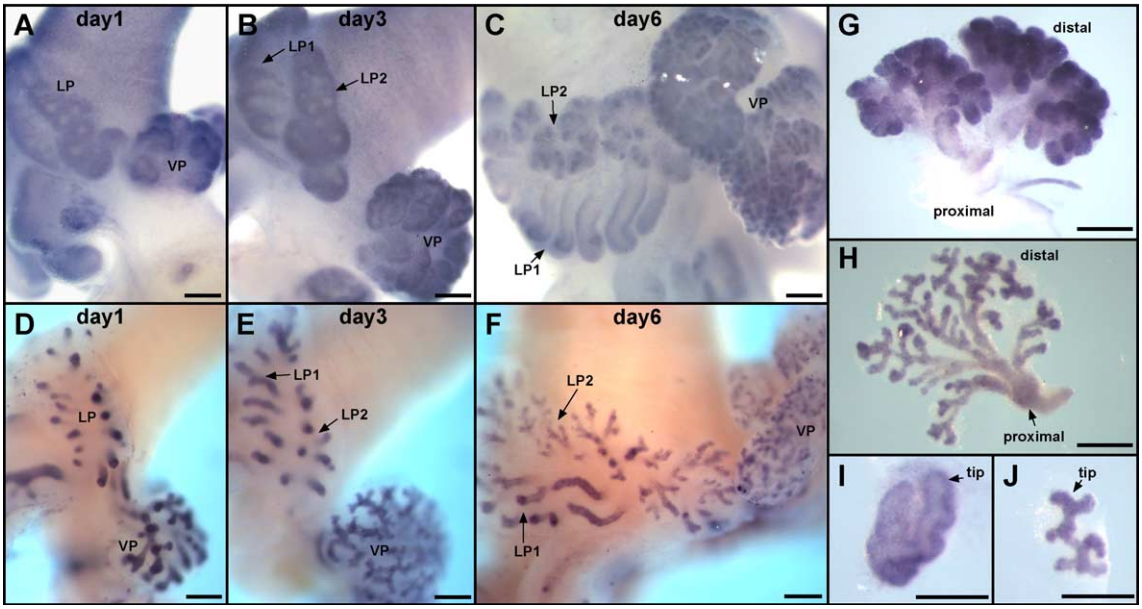

Fig. 1. Whole mount ISH for *Fgf*10 (A, B, C, G, and I) and *Fgf*R2*iii*b (D, E, F, H, and J) in the developing rat prostate gland. For each probe, the tissues on the different days were processed together to allow direct comparisons of signal strength. On pnd 1 (A), *Fgf*10 mRNA is broadly expressed in the DP and LP mesenchyme, whereas in the VP, mesenchymal *Fgf*10 has begun to coalesce in the condensed mesenchyme surrounding the elongating ductal buds in the distal aspects of the gland. At pnd 3 (B), intense *Fgf*10 expression is observed in the distal regions of all lobes and is approximate to the elongating and branching ducts. By pnd 6 (C), *Fgf*10 mRNA signal intensity has declined and is localized strictly to the condensed mesenchyme surrounding the elongating and branching ducts. A dissected pnd 6 VP sublobe (G) and distal tip (I) confirms the distal and periductal *Fgf*10 expression in the prostatic mesenchyme. In contrast, *Fgf*R2*iii*b expression was confined to the epithelial cells in the central-to-distal regions of the elongating ducts with the greatest expression at the distal tips from pnd 1 to 6 (D–F). A dissected pnd 6 VP sublobe (H) and distal tip (J) confirm that *Fgf*R2*iii*b is expressed exclusively in the epithelium with the most intense signal at the distal tips of the elongating and branching ducts. Each tissue is representative of 3–5 experiments. VP = ventral prostate, DP = dorsal prostate, LP = lateral prostate. Scale bar = 200 μm.

Fgf10 promotes prostatic ductal elongation and branching and enhances epithelial differentiation

To further clarify the roles for *Fgf*10 in prostate development, several organ culture experiments were performed. VP and LP prostate lobes were removed on pnd 0 and cultured for 6 days in testosterone with or without exogenous *Fgf*10 protein. For both lobes, the addition of *Fgf*10 enhanced prostatic growth and led to a cystic appearance at the distal tips of the prostatic ducts (Fig. 3A). This resulted in a modest increase in lobe area that was significant for the LP only (Fig. 3B). However, it is important to note that testosterone and endogenous *Fgf*10 were present in both culture groups. Cross-sectional analysis of the cultured tissues confirmed that the *Fgf*10-treated ducts were wider than the controls (Fig. 3D) at the nonlumenized distal aspects and were filled with cells (Fig. 3E), suggesting increased epithelial cell number as a result of *Fgf*10 treatment. This was confirmed by BrdU labeling that revealed that epithelial proliferation rates in the central–distal ducts of the *Fgf*10-treated LPs were significantly higher than testosterone controls (Fig. 3C). In contrast, proliferation rates in the proximal ducts were unaffected by *Fgf*10 exposure. It is noteworthy that the increased epithelial proliferation was confined to the central–distal ductal regions where *Fgf*R2*iii*b is present, implicating a direct effect of *Fgf*10 on epithelial cell proliferation.

Evidence was also observed for the enhancement or acceleration of prostatic epithelial differentiation by *Fgf*10. Prostate sections from the above cultures in testosterone with or without *Fgf*10 were labeled for basal cells using p63 and examined histologically. In LPs cultured in testosterone for 6 days, nonlumenized ducts were lined with a continuous layer of basal cells along the basement membrane and solid cords of early differentiating lumenal cells were piled above (Figs. 3D and F). In LPs cultured with testosterone plus *Fgf*10, the proximal–central ducts were consistently lumenized with differentiated columnar epithelium positioned above the basement membrane (Figs. 3E and G).

To directly examine the role of *Fgf*10 on ductal elongation and branching, mesenchyme-free prostatic ducts were isolated from the distal portion of the VP on pnd 0 and cultured for 44 h in growth factor-reduced Matrigel in the

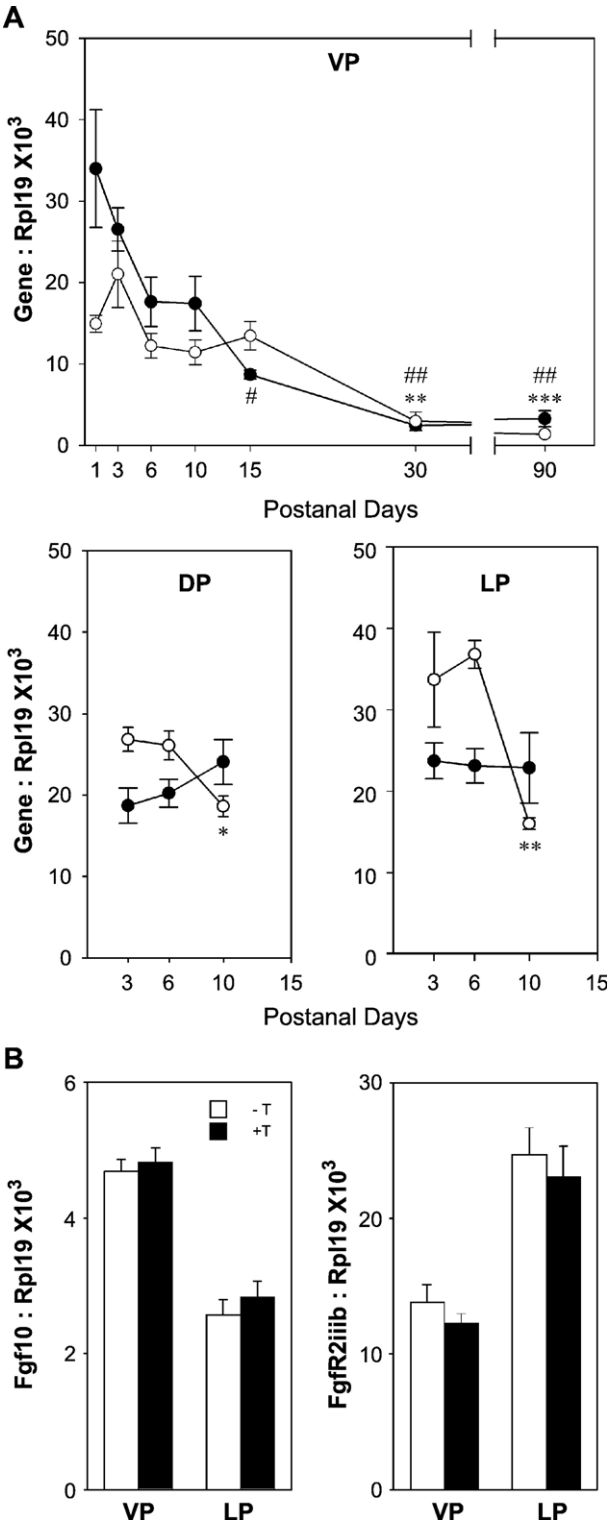

Fig. 2. (A) Ontogeny of *Fgf*10 and *Fgf*R2*iii*b mRNA expression in the rat prostate lobes as quantitated by real-time RT-PCR. *Fgf*10 (solid circles) expression in the VP was high at birth and significantly declined thereafter reaching a nadir by pnd 30 where it remained through adulthood. *Fgf*10 expression levels in the LP and DP in the early developmental stage are comparable with the levels in the VP. *Fgf*R2*iii*b (open circles) expression level peaked at pnd 3 in the VP and declined quickly thereafter reaching a stable low level at pnd 30. For DP and LP, *Fgf*R2*iii*b expression significantly declined by pnd 10 despite the fact that the epithelial cell number, where the receptor is expressed, was concomitantly increasing. Points represent mean ± SEM for 3–10 replicates. For VP *Fgf*10 level: $^{\#}P <$ 0.05 vs. pnd 1, $^{\#\#}P < 0.01$ vs. pnd 1. For VP *Fgf*R2*iii*b level: $^{**}P < 0.01$ vs. pnd 3, $^{***}P < 0.001$ vs. pnd 3. For LP and DP *Fgf*R2*iii*b level: $^{*}P <$ 0.05 vs. pnd 6, $^{**}P < 0.01$ vs. pnd 6. (B) Effect of testosterone (T) on *Fgf*10 and *Fgf*R2*iii*b mRNA expression in early prostate development. VPs and LPs were cultured for 20 h in the presence or absence of 10 nM testosterone. No significant differences in *Fgf*10 or *Fgf*R2*iii*b transcript levels were detected in either lobe. Bars represent mean ± SEM for eight replicates.

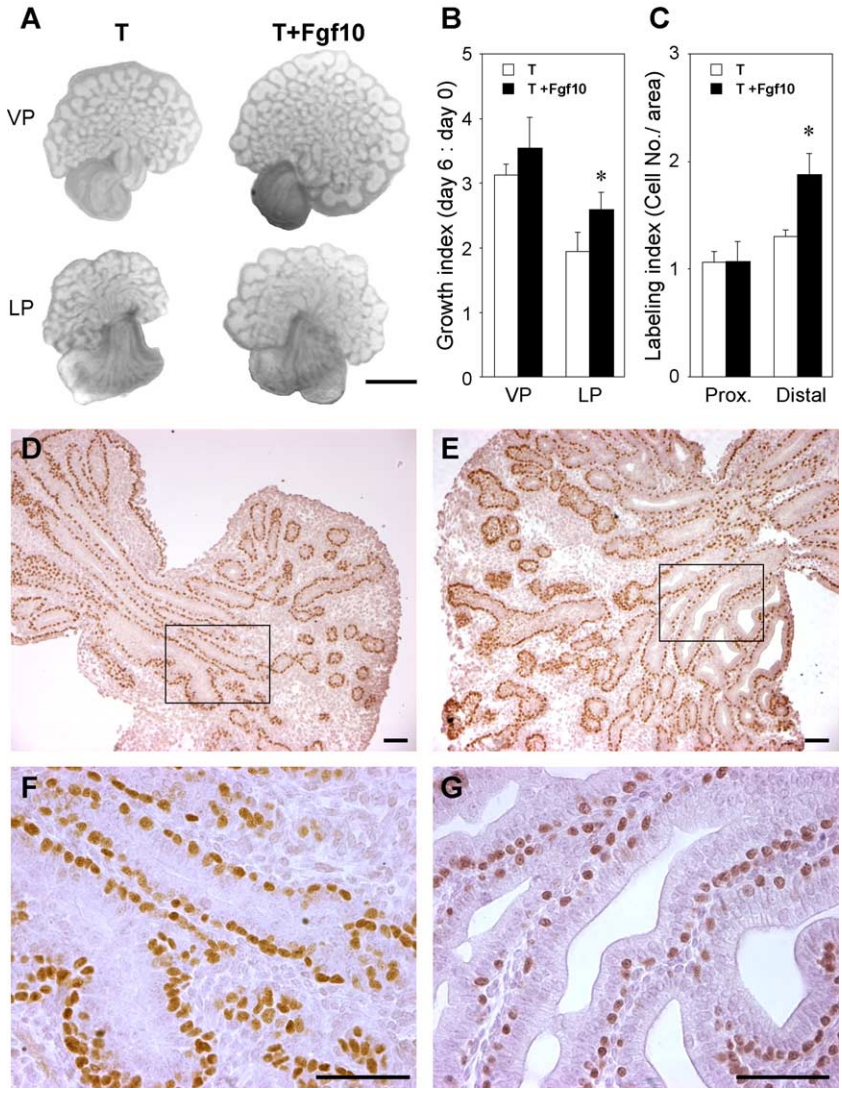

Fig. 3. Cultured VP and LP following application of *Fgf*10 or BSA. Paired lobes from a single rat were treated with either BSA or *Fgf*10 to allow direct comparison of *Fgf*10 treatment. (A) VPs (top) and LPs (bottom) cultured for 6 days in the presence of testosterone (T) and either BSA (left) or *Fgf*10 protein. *Fgf*10 addition enhanced ductal growth in both lobes and led to a cystic appearance at the distal ductal tips. (B) Growth index of VPs and LPs cultured for 6 days in the presence of T or T + *Fgf*10. 2D area on day 6 was normalized to day 0 area and bars represent the mean ± SEM of six replicates. While *Fgf*10 treatment augmented growth in both lobes, the difference was significant for the LP only (*$P < 0.05$). (C) Epithelial cell BrdU labeling index in LP cultured for 6 days with T alone or T + *Fgf*10. The bar represents the mean ± SEM of seven replicates. Proliferation was similar in the proximal ducts in both treatment groups whereas *Fgf*10 significantly (*$P < 0.05$) increased epithelial proliferation in the central–distal ducts. (D–G) Immunocytochemistry for p63 (basal cell marker) in LPs cultured for 6 days in T alone (D and F) or T + *Fgf*10 (E and G). Images in F and G are high power views of boxed areas in D and E, respectively. In LPs cultured in T alone, nonlumenized ducts throughout the lobe were lined with a continuous basal cell layer along the basement membrane and early differentiating lumenal cells filled the ducts (D and F). In LPs cultured in T + *Fgf*10 (E and G), ductal elongation and branching were more extensive than in T alone and lumen diameters appeared thicker. In addition, lumenization in the proximal ducts was consistently observed (E) and epithelial cytodifferentiation in those regions was complete with short columnar lumenal cells containing basally located nuclei and supranuclear clears zones positioned above an intermittent layer of p63-stained basal cells (G). Scale bar in A = 500 μm; in D–G = 50 μm.

presence of testosterone or *Fgf*10. Ducts grown in the presence of testosterone alone slowly balled up over the course of 44 h and exhibited no clefting, branching, or elongation, proving an absolute requirement of paracrine growth factors for this activity (Fig. 4A). Addition of 0.5 μg/ml *Fgf*10 to the medium increased ductal clefting and budding within 20 h and resulted in ductal elongation and increased thickness after 44 h (Figs. 4B,C). A dose response to exogenous *Fgf*10 was examined with increasing doses from 1 ng to 1 μg/ml, and effects on branching were not observed below 0.1 μg/ml (data not shown). *Fgf*R2*iii*b is a receptor tyrosine kinase that acts through the *ras/raf/Mek* pathway as well as the PLCγ/DAG/Ca^{++} pathways. To determine which pathway may be mediating prostatic ductal growth and budding, prostatic ducts were incubated with *Fgf*10 + U0126, a *Mek* inhibitor, and a complete blockade of *Fgf*10-induced budding and elongation was consistently observed (Fig. 4D). Thus, these results confirm that *Fgf*10

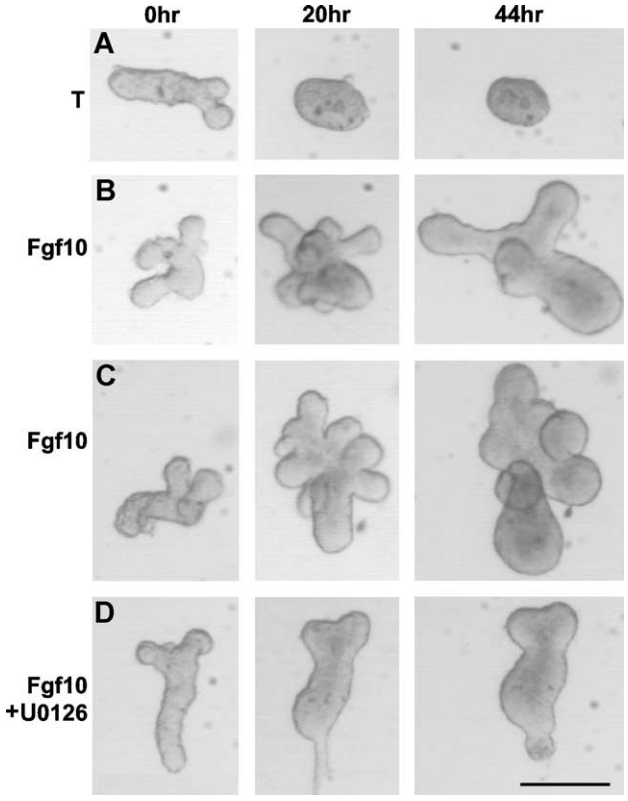

Fig. 4. Mesenchyme-free VP ductal cultures at 0, 20, and 44 h in the presence of 10^{-8} M testosterone (T), 0.5 μg/ml *Fgf*10, or 0.5 μg/ml *Fgf*10 + 20 μM U0126. With T alone (A), ducts slowly balled up over the course of 44 h and exhibited no growth. With *Fgf*10 addition (B and C), the ducts exhibited increased clefting and budding within 20 h. Ductal elongation and increased thickness, but no further budding was observed at 44 h. Addition of *Mek* inhibitor U0126 completely blocked the *Fgf*10-induced budding and elongation (D). Scale bar = 200 μm.

plays a direct role in stimulating prostatic duct elongation and branching that is mediated through the *ras/raf/Mek* pathway.

Fgf10 regulates the expression of prostatic morphogens and homeobox genes

To determine downstream genes of *Fgf*10 in the prostate gland, pnd 0 VPs were cultured for 24 h in the absence or presence of *Fgf*10 and the expression of several known prostatic morphogens and homeobox genes was quantified by real-time RT-PCR. Since we recently showed that *Shh* downregulated prostatic *Fgf*10 within 18 h (Pu et al., 2004), we first examined whether *Fgf*10 in turn affects *Shh* expression to form a feedback loop. As shown by wmISH (Figs. 5A–B) and RT-PCR (Fig. 5C), *Fgf*10 significantly upregulates epithelial *Shh* expression within 24 h. Further, the mesenchymal *Shh* receptor *ptc* was also upregulated by *Fgf*10 exposure, most likely mediated through elevated levels of the secreted *Shh*, a known inducer of its receptor. In addition, *Bmp*4, a prostatic mesenchymal gene upregulated by *Shh* (Pu et al., 2004), was significantly repressed following *Fgf*10 treatment. The expression of *Fgf*R2*iii*b was not affected by *Fgf*10 treatment, thus autoregulation of its cognate receptor is not an action of *Fgf*10 in the prostate gland. *Bmp*7, a secreted epithelial morphogen (Huang et al., 2003), was markedly upregulated by *Fgf*10 within 24 h. Further, two epithelial homeobox genes known to be involved in prostate epithelial differentiation, *Nkx*3.1 and *Hox*b13, were rapidly upregulated following *Fgf*10 exposure. These data strongly implicate *Fgf*10 as an important regulator of growth factor networks and homeobox genes critical for prostate branching morphogenesis and differentiation.

Neonatal estradiol exposure suppresses Fgf10, FgfR2iiib, and Bmp7 in a lobe-specific manner

We previously determined that neonatal exposure to estradiol results in lobe-specific phenotypes with greater branching deficiencies in the LP and DP and a high incidence of adult-onset dysplasia in the VP (Prins, 1997; Pu et al., 2004). Furthermore, we recently demonstrated that the DP/LP branching deficiencies were due, in part, to lobe-specific reduction in *Shh-ptc-gli* expression (Pu et al., 2004). In the present study, exposure to estradiol on pnd 0, 3, and 5 similarly reduced *Fgf*10 and *Fgf*R2*iii*b in the LP and *Fgf*R2*iii*b in the DP but had no effect on the expression of these two genes in the VP. As early as pnd 1, wmISH consistently revealed suppression of *Fgf*R2*iii*b in the LP regions whereas *Fgf*10 suppression was noticeable by pnd 3 when tissues from control and estrogen-treated rats were processed together (Figs. 6A–D) while gene expression was similar between the two groups in the VP. The suppression of *Fgf*10 and *Fgf*R2*iii*b expression in the LP and to a lesser extent the DP persisted through pnd 6 and correlated with a blunting of ductal elongation and branching in those regions (Figs. 6E and F). These findings were quantitatively corroborated by real-time RT-PCR that revealed no differences between treatment groups for *Fgf*10 and *Fgf*R2*iii*b mRNA levels in the VP between pnd 1–90 (Fig. 7A). In contrast, LP expression of *Fgf*10 was significantly lower at pnd 3 and 6, and *Fgf*R2*iii*b was markedly reduced at pnd 6 and 10 in estrogen-treated rats as compared to controls (Fig. 7C). In the DP, *Fgf*10 expression was not affected by estrogen exposure but *Fgf*R2*iii*b was significantly reduced at pnd 6 and 10 (Fig. 7B). Thus, *Fgf*10 signaling is disrupted in both the DP and LP lobes following estrogenization with the greatest impact observed in the LP. Since the two genes are expressed in different tissue compartments, altered ratios of stroma/epithelium following neonatal estrogen exposure cannot account for the decline in expression of both genes.

Immunocytochemistry was used to examine the *Fgf*10 and *Fgf*R2*iii*b protein levels in the developing LP and VP following estrogen treatment, and the findings correlated with the transcript levels. In the control LP and VP, *Fgf*10 protein localized to the stroma in the distal aspects of the glands as well as the epithelial cells where it is known to

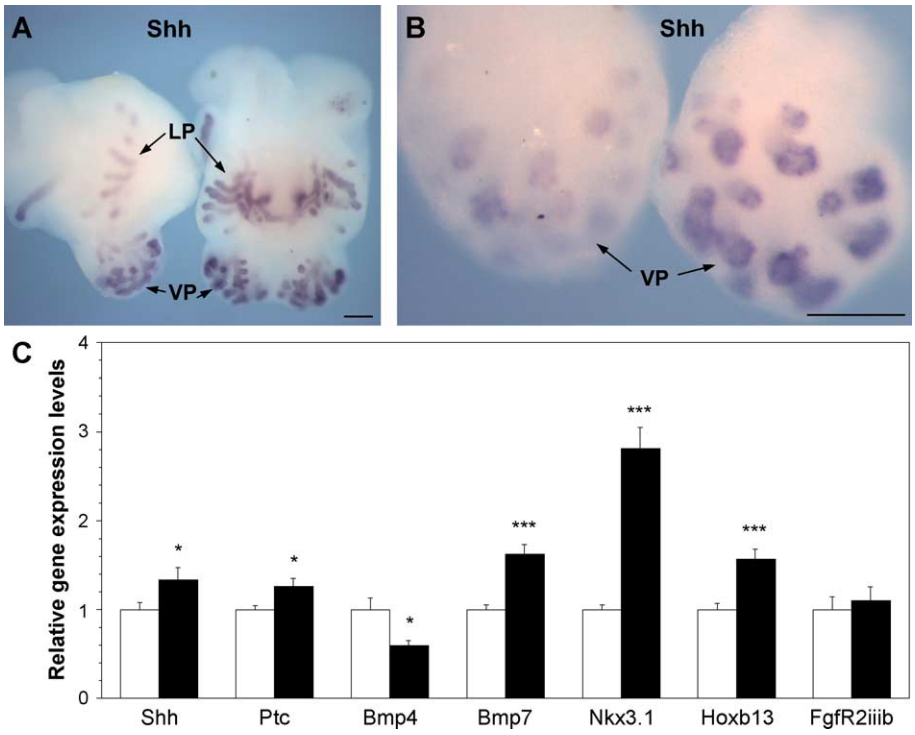

Fig. 5. The effects of *Fgf*10 on prostatic gene expression. (A) Whole mount ISH of *Shh* mRNA in the pnd 0 UGS–prostatic complex following culture for 24 h in BSA (left) or 0.5 μg/ml *Fgf*10 (right). Samples shown were processed together to allow direct comparison of signal intensity. *Fgf*10 significantly upregulated epithelial *Shh* expression in the VP and LP ducts within 24 h. Scale bar = 200 μm. (B) A higher power view of VPs from a replicate set of tissues exposed to BSA (left) or 0.5 μg/ml *Fgf*10 (right) for 24 h followed by wmISH for *Shh* mRNA. *Shh* signal intensity is visibly higher in the distal tips of VP ducts following *Fgf*10 exposure. Both VPs were processed together to allow direct comparison of signal intensity. Scale bar = 200 μm. (C) Gene expression as determined by real-time RT-PCR from contralateral VPs ($n = 8$) cultured in the presence of BSA (open bars) or 0.5 μg/ml *Fgf*10 protein (solid bars) for 24 h. The mRNA level for each gene following *Fgf*10 exposure is expressed relative to BSA control levels (determined as 1) following initial quantitation and normalization to Rpl19 levels. *Fgf*10 significantly increased epithelial *Shh* and mesenchymal *ptc* expression, suppressed mesenchymal *Bmp*4 expression, and markedly increased epithelial *Bmp*7, *Nkx*3.1, and *Hox*b13 expression as compared to BSA controls. The expression of *Fgf*R2*iii*b expression was not altered by *Fgf*10 treatment. Bars represent the mean ± SEM for eight replicates. $*P < 0.05$, $***P < 0.001$, *Fgf*10 vs. BSA controls.

bind to its receptors (Figs. 8A and C). Following estrogen treatment, there was a marked decline in *Fgf*10 protein in the LP (Fig. 8B), whereas protein staining in the VP was equivalent to that observed in oil-treated controls (Fig. 8D). *Fgf*R2*iii*b was initially localized to the cytoplasm of undifferentiated prostate epithelial cells on days 1 and 3 (data not shown), and additional immunostain was observed in the epithelial cell nuclei of the LP and VP by pnd 6 (Figs. 8E and G). This immunostain was reduced in intensity throughout the DP and LP ducts following estrogen exposure (Fig. 8F) but was unaltered by hormone treatment in the VP (Fig. 8H).

Since the above findings showed that *Bmp*7 is downstream of *Fgf*10 in the prostate, we examined the response of this gene to *Fgf*10 and *Fgf*R2*iii*b downregulation following estrogen exposure as a functional marker for *Fgf*10 action. *Bmp*7 was localized by wmISH to epithelial cells in the distal tips of the elongating ducts on pnd 1, and its expression markedly increased by pnd 3 as the ducts entered the active phase of branching morphogenesis (Figs. 9A–C). Following neonatal estradiol exposure, *Bmp*7 expression was significantly suppressed in the DP and LP lobes but was not affected in the VP as revealed by wmISH (Figs. 9A and B) and real-time RT-PCR analysis (Fig. 9D). This lobe-specific *Bmp*7 suppression that mirrors the decrease in *Fgf*10/*Fgf*R2*iii*b expression in the DP and LP suggests that downregulation of *Fgf*10 signaling may be the proximate cause of estrogenized defects in the dorsolateral lobe.

Direct effects of estradiol on Fgf10 and FgfR2iiib expression

To determine whether the effects of estradiol on prostatic *Fgf*10 and *Fgf*R2*iii*b expression were direct prostatic effects or indirectly mediated through systemic alterations following estrogen treatment, an organ culture system was employed for the developing LP. On the day of birth, LPs were removed from the prostatic/UGS complex and grown in vitro with testosterone or testosterone plus 20 μM estradiol (contralateral lobes). As shown in Fig. 10A, the LP ductal growth and branching that occurred in the presence of testosterone over 6 days were markedly suppressed by the addition of estradiol, indicating that the estrogen effects were directly mediated at the prostatic level. Furthermore, measurement of *Fgf*10 and

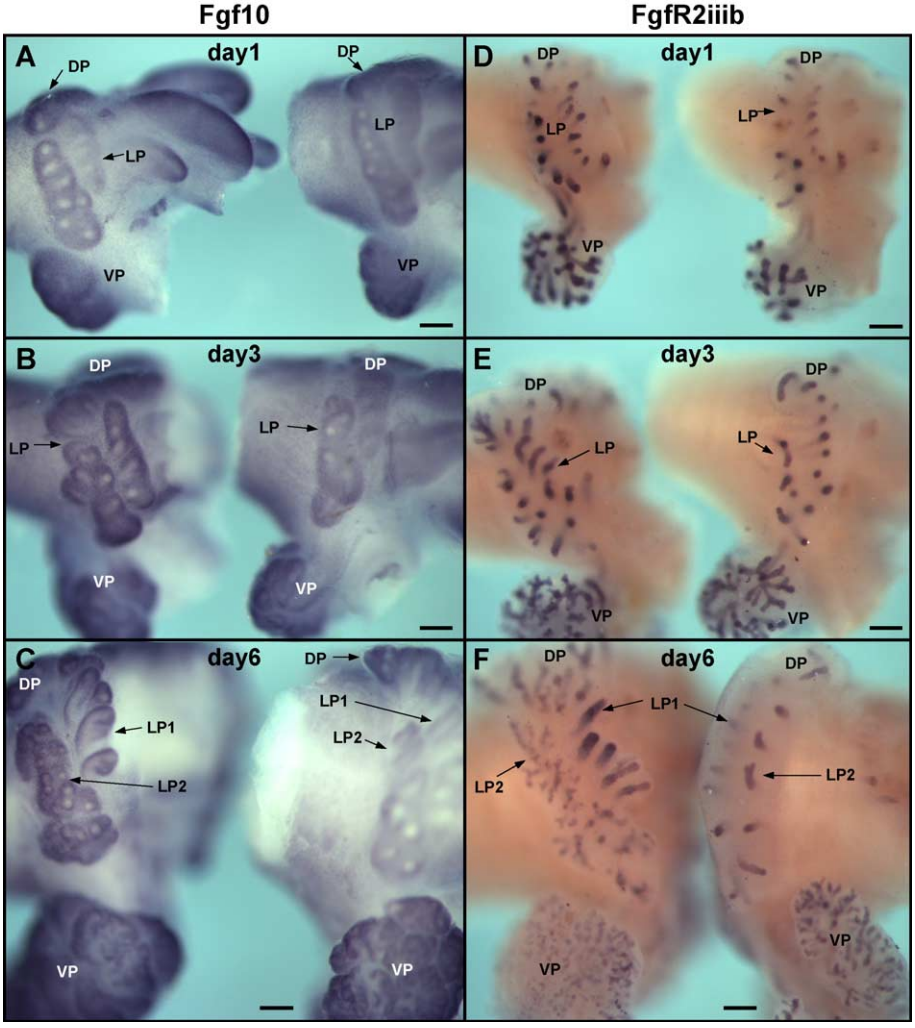

Fig. 6. Whole mount ISH (wmISH) for *Fgf*10 (A–C) and *Fgf*R2*iii*b (D–F) expression in the UGS–prostatic complexes from control and estrogen-exposed rats. Treated tissues for each probe were processed and photographed together to allow direct comparisons of signal intensity between treatment groups. (A) *Fgf*10 message in pnd 1 oil (left) and estradiol-treated (right) rats. Mesenchymal *Fgf*10 signal intensity was lower in estrogen-exposed LPs as compared to oil-treated controls while the signal in the VPs appeared unaffected. (B and C) *Fgf*10 transcript in pnd 3 (B) and pnd 6 (C) prostates from rats treated with oil (left) or estradiol (right). Mesenchymal *Fgf*10 expression in the distal regions of the LPs was markedly suppressed by estrogen exposure as compared to oil-treated controls while expression in the VP was unaffected. (D) *Fgf*R2*iii*b transcript in pnd 1 complexes from control (left) and estrogen-treated rats (right). Signal intensity for *Fgf*R2*iii*b transcript at the distal tips of elongating ducts was markedly reduced in the estrogen-exposed LP and DP as compared to controls while VP expression appeared minimally affected by estrogen treatment. (E and F) *Fgf*R2*iii*b wmISH in pnd 3 (E) and 6 (F) prostatic complexes from control (left) and estrogen-exposed rats (right). Ductal growth, branching, and *Fgf*R2*iii*b expression were markedly reduced in the LPs and DPs of rats exposed to estradiol as compared to controls while VP expression remained unaffected. Each tissue is representative of 3–5 experiments. Scale bar = 200 μm.

*Fgf*R2*iii*b transcript levels in cultured LPs by real-time RT-PCR showed a significant reduction in the expression of both genes, indicating that altered expression of these genes is a direct result of estrogen exposure (Fig. 10B). The reduction in epithelial *Fgf*R2*iii*b expression was visualized by wmISH (Fig. 10C), where DLP, but not VP, signal was markedly lower following culture in estradiol.

Fgf10 restores ductal growth and branching in LPs exposed to estradiol in vitro

To determine whether reduced prostatic *Fgf*10 signaling mediates the suppression of LP branching morphogenesis in response to estrogen exposure, organ culture experiments were undertaken with exogenous *Fgf*10 replacement. LPs were removed on the day of birth and cultured with testosterone (T), testosterone plus 20 μM estradiol (T + E_2), or testosterone plus estradiol and 0.5 μg/ml *Fgf*10. As shown in Fig. 11A, LPs cultured in the presence of estradiol (T + E_2) showed marked inhibition of ductal elongation and branching as compared to LPs cultured in the presence of testosterone alone. The addition of *Fgf*10 to the T + E_2 culture fully rescued LP growth and branching, which were confirmed by measurement of prostatic area (Fig. 11B). Histological examination revealed stunted epithelial ducts filled with undifferentiated epithelial cells following in vitro estradiol

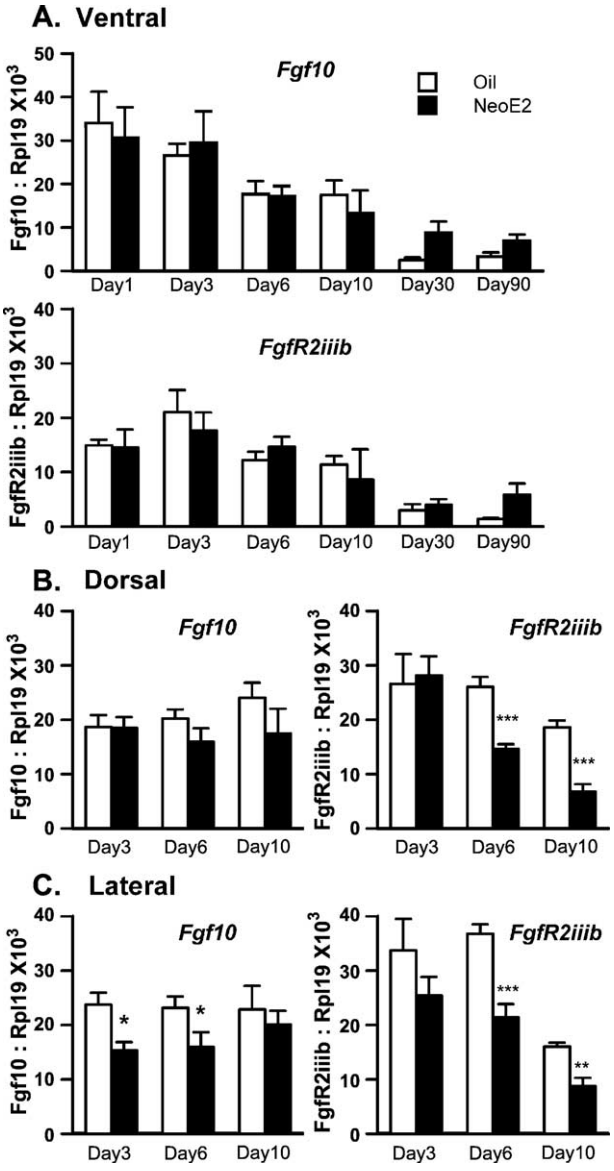

Fig. 7. Real-time RT-PCR of *Fgf*10 and *Fgf*R2*iii*b mRNA levels over time in the (A) VP, (B) DP, and (C) LP of control (open bars) and estrogen-exposed rats (solid bars). Expression of both genes in the VP at all time points was not influenced by neonatal estrogen exposure. Estrogen exposure resulted in a significant decrease in *Fgf*10 expression in the LP at pnd 3 and 6, and a significant decrease in *Fgf*R2*iii*b expression in the LP and DP at pnd 6 and 10. Bars represent the mean ± SEM for 3–10 replicates per treatment and time point. $*P < 0.05$, $**P < 0.01$, $***P < 0.001$ estrogen-treated vs. controls at specific time points.

exposure (Fig. 11C). The addition of *Fgf*10 to the T + E_2 culture reversed the estrogen suppression of cellular differentiation and LPs resembled those cultured in testosterone alone or testosterone + *Fgf*10 (Figs. 3D–G). Taken together, these data provide compelling evidence that *Fgf*10 and its downstream genes are able to restore growth and branching to estrogen-exposed LPs and support the hypothesis that alterations in the *Fgf*10/*Fgf*R2*iii*b pathway are involved in mediating the estrogenized phenotype.

Discussion

Fgf10 and FgfR2iiib localize to the distal signaling center in the developing rat prostate lobes

The present study provides a clear spatiotemporal picture of the expression patterns of Fgf10 and FgfR2iiib in separate rat prostate lobes during development. As has been previously described for the rat VP (Thomson and Cunha, 1999), Fgf10 is broadly expressed in distal mesenchymal cells of all lobes as prostatic buds emerge from the UGS at the time of birth. As the ducts elongate and make contact with this Fgf10 expression domain, the pattern shifts such that the highest expression is observed in the condensed mesenchyme immediately surrounding the distal ducts while interductal Fgf10 expression declines. In this manner, Fgf10-expressing cells make direct contact with the basement membrane ECM surrounding the elongating epithelial ducts at the time when branching commences. This was substantiated by immunolocalization of the secreted Fgf10 protein that was observed in the distal periductal mesenchyme and along the basal aspects of the ductal epithelium where it is known to ligand to its receptor FgfR2iiib. This shift to a periductal expression pattern occurs ~2 days later for the DP and LP than for the VP, consistent with the known time delay in branching morphogenesis for these more anterior lobes (Hayashi et al., 1991).

Previous reports on the localization of FgfR2iiib have shown that it is exclusively expressed by prostatic epithelium, thus establishing the paracrine nature of this morphoregulatory signal (Finch et al., 1995). In the present study, we characterize this further through the use of wmISH and ICC, and demonstrate that FgfR2iiib is localized to the far centro-distal region of the elongating and branching ducts and is absent in the proximal and initial central prostatic ducts. Thus, similar to Shh in the developing prostate (Pu et al., 2004), Fgf10 action through FgfR2iiib is highest in the distal signaling center at the ductal tips during the active phase of branching morphogenesis. This regionalized paracrine function for Fgf10 is supported by BrdU labeling results following exogenous Fgf10 exposure where epithelial cell proliferation increases in the centro-distal ducts while no additional proliferative response is noted in the proximal ducts. As branching morphogenesis nears completion in separate lobes (between days 6 and 15), expression levels for Fgf10 or FgfR2iiib decline, reaching their nadir at day 30 where they remain through adulthood confirming the primary role for this morphoregulatory factor in the developmental process.

While initial studies indicated that Fgf10 expression was upregulated by testosterone in prostatic stromal cells in vitro (Lu et al., 1999), organ culture studies indicated that androgen regulation of Fgf10 mRNA levels was nominal after 4 days of exposure (Thomson and Cunha, 1999). In the

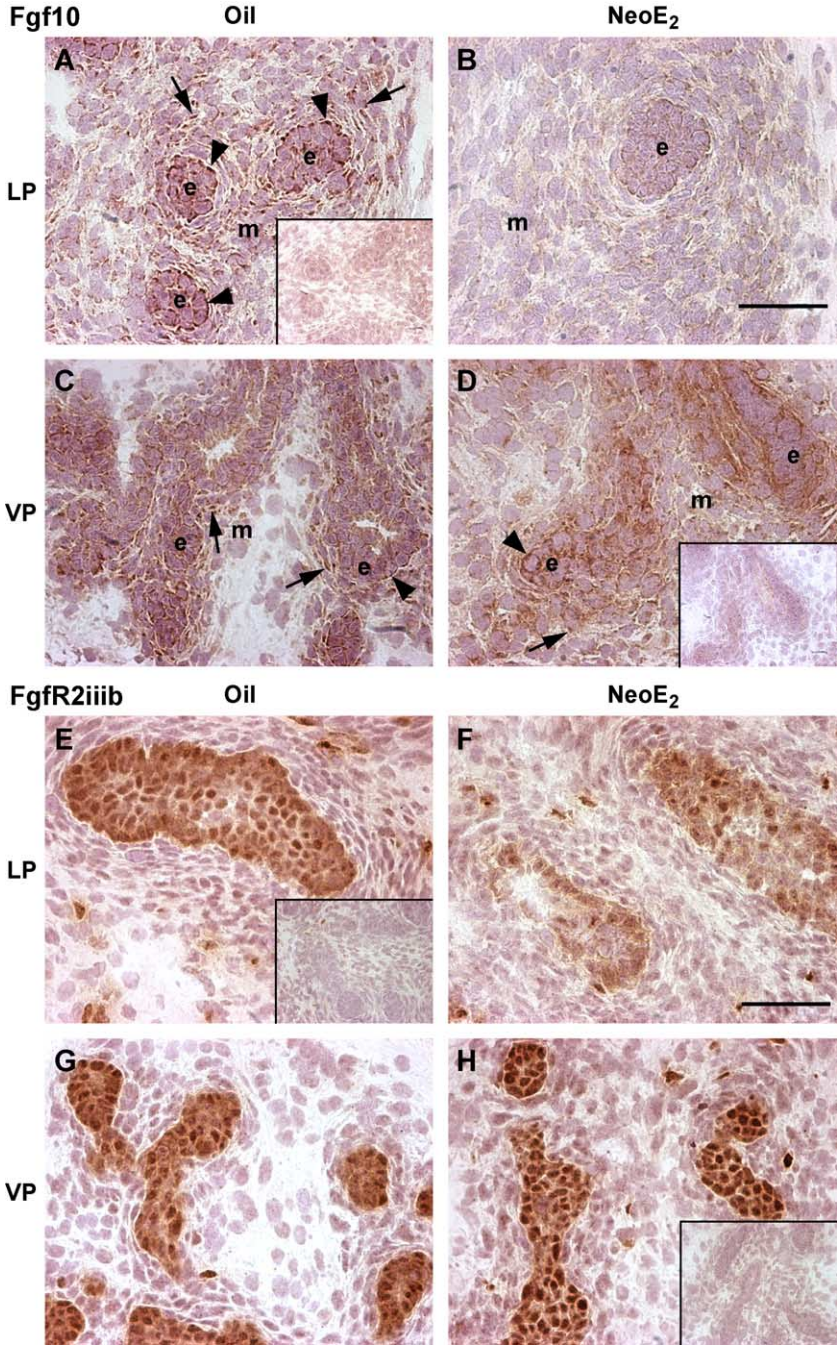

Fig. 8. Immunocytochemistry of *Fgf*10 and *Fgf*R2*iii*b protein in rat prostate at pnd 6. (A–D) *Fgf*10 protein in control (left) and estrogen-treated (right) LPs and VPs. In the control LP (A) and VP (C), *Fgf*10 protein localized to both mesenchymal cells (m, arrows) and the basal surface of epithelial cells (e, arrowheads) in the distal aspects of the glands. Following estrogen exposure, *Fgf*10 immunostaining was reduced in the LP (B) while protein staining in the VP was similar to that observed in the oil-treated controls (D). Inserts in A and D show normal goat-IgG-negative controls. (E–H) *Fgf*R2*iii*b protein in the distal tips of control (left) and estrogen-treated (right) LPs and VPs. In the control LP (E) and VP (G), *Fgf*R2*iii*b localized to epithelial cells in the distal aspects of the glands. Occasional stromal cells immunostained positive; however, this appeared in the normal goat-IgG-negative controls (E, inset), suggesting nonspecificity. Following estrogen exposure, *Fgf*R2*iii*b immunostain was reduced in the LP (F) while the protein staining in the VP was similar to that observed in oil-treated controls (H). Scale bar = 50 μm.

present study, we tested whether testosterone could affect whole prostate Fgf10 transcript levels prior to changes in cellular composition as a result of androgen exposure. We find that testosterone has no effect on Fgf10 expression in the rat VP or LP within 20 h of exposure, which confirms that this is not an androgen-regulated gene in the prostate in situ. Furthermore, we demonstrate that testosterone does not affect FgfR2iiib expression, which, in total, indicates that androgens do not directly affect Fgf10 signaling in the developing prostate gland.

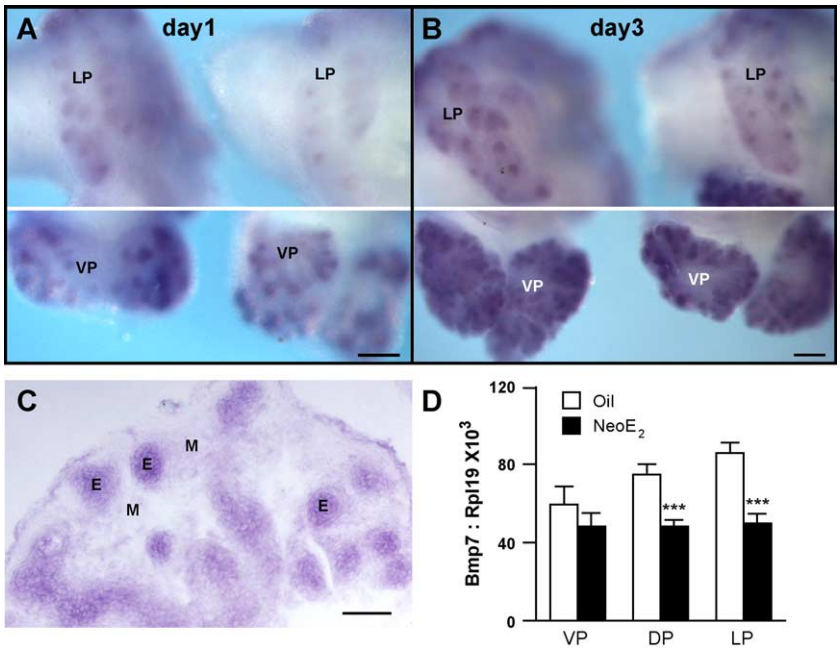

Fig. 9. *Bmp*7 expression in the developing prostate. (A) Whole mount ISH for *Bmp*7 in the UGS–prostatic complexes from control (left) and estrogen-exposed rats (right) on pnd 1. An image of the dorsolateral region is shown in the top panel, while VPs from the same tissue are shown in the bottom panel at a separate focal plane. Both tissues were processed together to allow direct comparisons of signal intensity. *Bmp*7 transcript is localized to the distal tips of the ducts and is visibly suppressed in the DLP but not the VP by estrogen exposure. Scale bar = 200 μm. (B) *Bmp*7 transcript in pnd 3 prostates from rats treated with oil (left) or estradiol (right). The *Bmp*7 signal is more intense in all lobes of the pnd 3 control rat as compared to pnd 1. In the estrogen-treated rat, the LP (top) signal is reduced while the VP (bottom) signal is similar to that observed in control tissues. The tissues in A and B were processed together to allow direct comparison of signal intensity and this result was repeated five times. Scale bar = 200 μm. (C) Cross-section wmISH shows the epithelial localization of *Bmp*7 at the distal tips of the VP. E = epithelial, M = mesenchyme. Scale bar = 50 μm. (D) Real-time RT-PCR of *Bmp*7 on pnd 6 of control (open bars) and estrogen-exposed rats (solid bars). Estrogen significantly reduced *Bmp*7 expression in the DP and LP while VP expression levels were unaffected. Bar represents the mean ± SEM of 7–10 replicates. **P* < 0.001, estrogen-treated vs. controls.

Role of Fgf10 in branching, ductal growth, epithelial proliferation, and differentiation

Previous studies with rodents have shown an essential role for *Fgf*10 in both prostatic bud induction (Donjacour et al., 2003) and ductal branching (Thomson and Cunha, 1999). The present study confirms and extends this later role for *Fgf*10 during prostate development. We observe that exogenous *Fgf*10 augments testosterone-induced prostatic growth in LP and, to a lesser degree, VP organ cultures by increasing epithelial cell proliferation in the distal but not proximal ductal regions. In this system, the terminal ducts appear cystic, which may be related to the uncontrolled availability of exogenous *Fgf*10 that can lead to growth and branching distortions, as was previously noted in the lungs (Cardoso, 2000). Our mesenchyme-free ductal culture studies demonstrate a direct role for *Fgf*10 in prostatic ductal elongation and branching. While testosterone alone is incapable of inducing ductal clefting or elongation in VP distal ducts grown in growth factor-reduced Matrigel, *Fgf*10 alone stimulates ductal clefting and branch points within 20 h and drives ductal elongation thereafter. In addition, inhibition of this process by a specific *Mek* inhibitor indicates that these activities of *Fgf*10 are mediated through the *ras/raf/Mek* pathway and not through the alternate PLCγ/DAG/Ca++ pathway (Szebenyi and Fallon, 1999). Together, these findings prove that *Fgf*10 is capable of directly initiating branch points and stimulating elongation of prostatic ducts. However, ductal branching to the full extent observed in vivo was not recapitulated with *Fgf*10 in vitro, which suggests that other growth factor pathways such as *Shh* (Pu et al., 2004) and *Bmp*7 (see below) are required for complete branching morphogenesis.

The organ culture studies also provide evidence that *Fgf*10 may be involved in prostate epithelial cell differentiation. Prostates grown in the presence of testosterone plus *Fgf*10 exhibited accelerated ductal lumenization and columnar epithelial cell differentiation as compared to lobes cultured in the presence of testosterone alone. Studies with the lung have shown a similar role for *Fgf*10 in epithelial differentiation in addition to its role as an inducer of branching (Cardoso, 2001; Peters et al., 1994). It is noteworthy that *Fgf*10 rapidly and significantly upregulated expression of *Nkx*3.1 and *Hox*b13, two homeobox genes preferentially expressed by the prostate epithelium that are involved in epithelial differentiation (Bhatia-Gaur et al., 1999; Economides and Capecchi, 2003; Prins et al., 2001a,b). Thus, it is possible that *Fgf*10 may influence epithelial differentiation, in part, through these downstream genes.

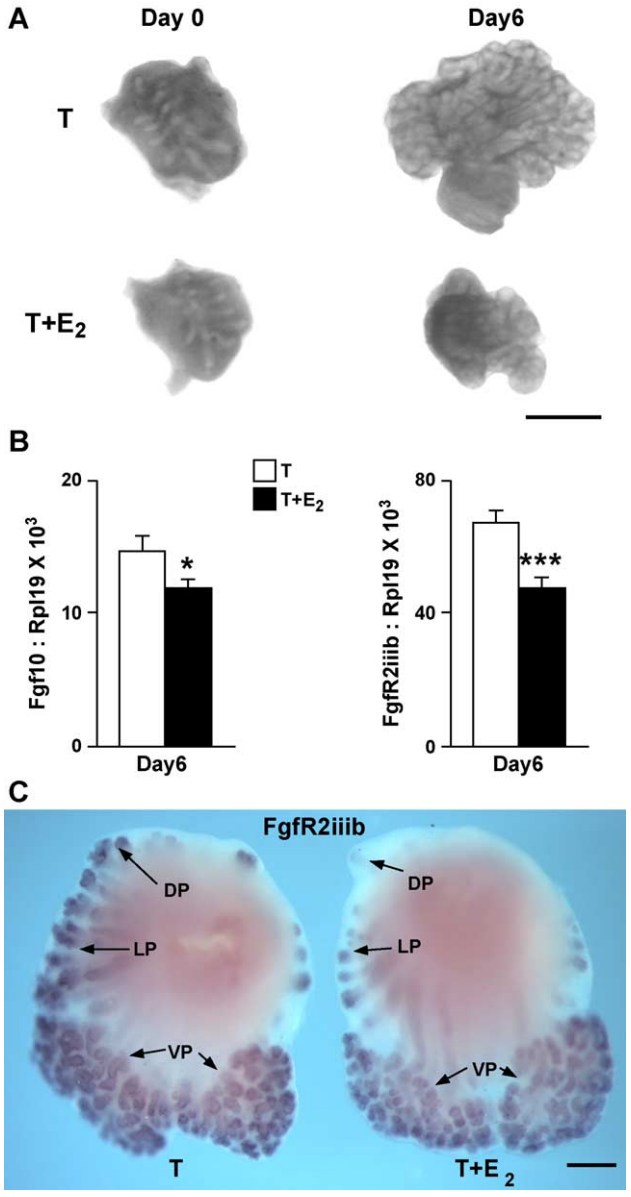

Fig. 10. (A) LPs collected on pnd 0 and cultured for 6 days in basal medium with 10^{-8} M testosterone (T) or with testosterone plus 20 μM estradiol (T + E_2). Ductal elongation and branching observed in day 6 T cultures were suppressed when LPs were cultured in T + E_2. Scale bar = 500 μm. (B) Real-time RT-PCR for *Fgf*10 and *Fgf*R2*iii*b in the LP after 6 days in culture with T (hatched bars) or T + E_2 (solid bars). Bars represent the mean ± SEM for 10 replicates. *$P < 0.05$, ***$P < 0.001$, T vs. T + E_2. (C) Whole mount ISH of *Fgf*R2*iii*b transcript in the pnd 0 UGS–prostatic complex after 40 h of culture. For photographic purposes, the complex was tilted to allow a clearer view of one side of the LP and DP. Epithelial *Fgf*R2*iii*b expression was decreased in the DP and LP cultured in T + E_2 (right) when compared with T alone (left) while expression in VP is not affected by estrogen treatment. This assay was replicated three times. Scale bar = 200 μm.

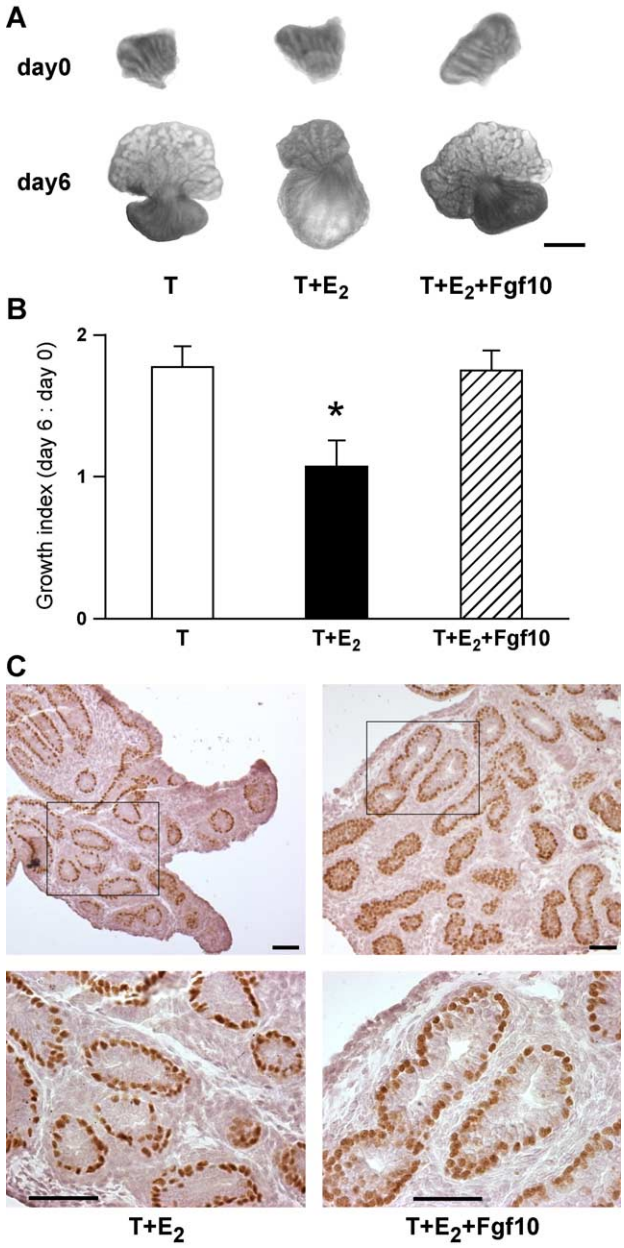

Fig. 11. *Fgf*10 restores ductal growth and branching in LPs exposed to estradiol in vitro. (A) LP cultured for 6 days in basal medium with 10^{-8} M testosterone (T), testosterone + 20 μM estradiol (T + E_2), and testosterone + estradiol + 0.5 μg/ml *Fgf*10 (T + E_2 + *Fgf*10). Top row, tissues at day 0; bottom row, tissues after 6 days of culture. LPs cultured in the presence of estradiol (T + E_2) showed marked inhibition of ductal elongation and branching as compared to LPs cultured in the presence of testosterone alone (T). The addition of *Fgf*10 to the T + E_2 culture (T + E_2 + *Fgf*10) fully rescued the LP growth and branching. Scale bar = 500 μm. (B) Prostatic 2D area in day 6 LPs normalized to day 0 area. Bars represent the mean ± SEM for six replicates. *$P < 0.05$, T + E_2 vs. T + E_2 + *Fgf*10. (C) Tissues from T + E_2 (left) and T + E_2 + *Fgf*10 (right) cultures shown in A were sectioned and immunostained for basal cell p63. The images on the bottom are high-powered views of boxed areas shown above at low power. The LPs cultured in T + E_2 were stunted and nonlumenized ducts were filled with early differentiated lumenal cells above a continuous layer of basal cells. The addition of *Fgf*10 to the T + E_2 cultures restored ductal elongation and branching and lumenized ducts with epithelial cytodifferentiation appeared in the proximal regions. Scale bar = 50 μm.

Downstream genes of Fgf10: signaling networks during rat prostate development

While *Fgf*10 is known to regulate the expression of signaling molecules in several developing branched struc-

tures (Cardoso, 2001; Haraguchi et al., 2000; Revest et al., 2001; Szebenyi and Fallon, 1999), downstream targets for *Fgf*10 action in the prostate gland have not been previously defined. Herein we demonstrate that *Fgf*10 has multiple downstream genes in the developing rat prostate gland including other signaling networks and homeobox genes that position this secreted morphogen as a key regulator of both prostate branching, growth, and differentiation. Epithelial *Shh* and its mesenchymal receptor *ptc* are upregulated by *Fgf*10 within 18 h of *Fgf*10 exposure, the later gene effect most likely being mediated through *Shh*, which autoregulates its receptor (Lamm et al., 2002). We have previously demonstrated that *Shh* locally downregulates *Fgf*10 expression in prostatic mesenchyme (Pu et al., 2004). As schematized in Fig. 12A, we propose that *Fgf*10, via epithelial *Fgf*R2*iii*b, directly upregulates epithelial *Shh* expression resulting in upregulation of mesenchymal *ptc* and *gli*s that downregulate mesenchymal *Fgf*10 expression, thus establishing a negative feedback loop that provides tight control of branching. In the limb bud, *Shh* was similarly identified as a downstream target of *Fgf*R2*iii*b (Revest et al., 2001); however, in that system, *Fgf*10 and *Shh* were found to induce each other (Ohuchi et al., 1997), which points out the specificity of growth factor cascades in different tissues.

The present studies further show that *Fgf*10 regulates prostatic expression of *Bmp* family molecules that have known roles in branching morphogenesis. In the submandibular gland, *Bmp*7 works together with *Fgf*7 and *Fgf*10 to promote branching morphogenesis while *Bmp*4 plays an opposing role that together control appropriate gland formation (Hoffman et al., 2002). While a similar role for

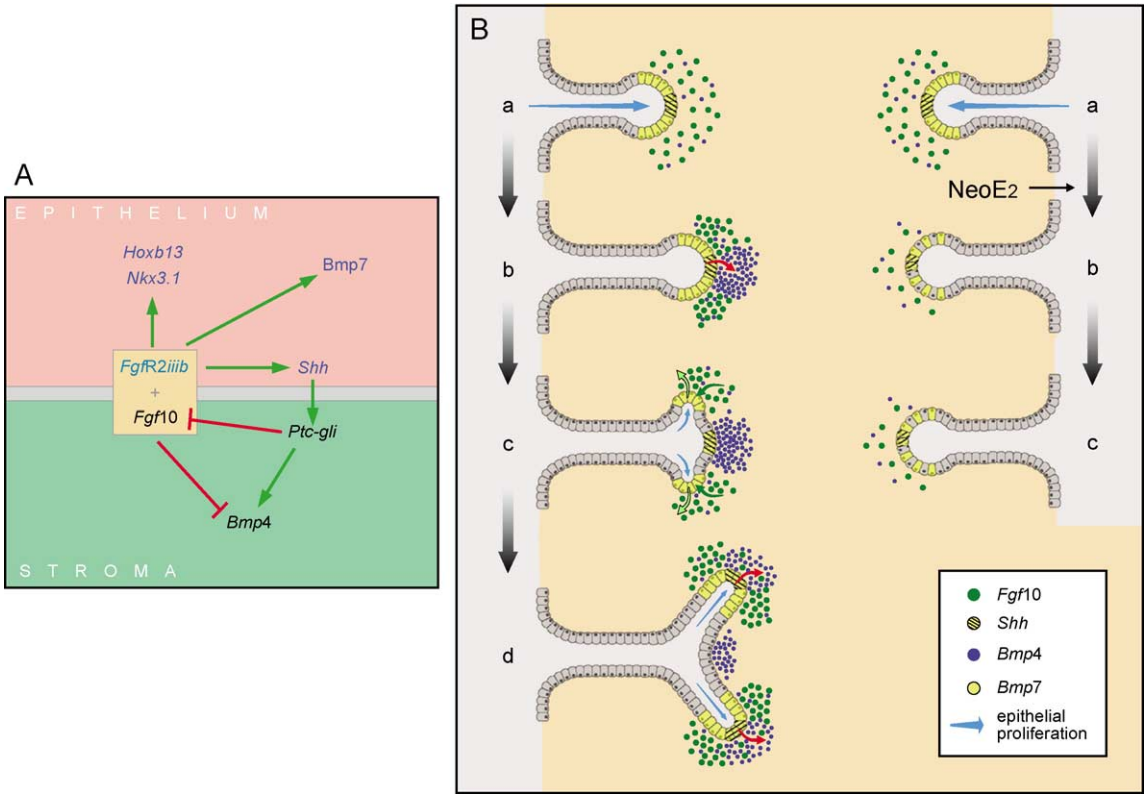

Fig. 12. (A) A schematic representation of regulatory networks between secreted morphogens in epithelial and mesenchymal cells at the distal signaling center of the developing prostate gland. *Fgf*10 (mesenchymal) and *Fgf*R2*iii*b (epithelial) upregulate (green arrows) epithelial expression of *Shh* and *Bmp*7 involved in branching morphogenesis as well as *Hox*b13 and *Nkx*3.1 involved in epithelial differentiation. *Shh* upregulates *ptc* and *gli* in adjacent mesenchymal cells that downregulate (red lines) *Fgf*10 expression, thus establishing a negative feedback loop for controlled growth. *Shh-ptc-gli* also upregulates the growth inhibitory *Bmp*4 molecule in the mesenchyme while *Fgf*10 downregulates its expression, which further serves to tightly control localized tissue growth. (B) The left side shows a tentative model for dichotomous branching of the developing rat prostate ducts as controlled by localized expression of secreted morphoregulatory factors. The distal signaling center of elongating epithelial buds expresses *Bmp*7 in all cells (yellow cells including yellow hatched cells) and *Shh* in discreet foci (yellow hatched cells only) while the distal mesenchyme expresses *Fgf*10 (green dots) and *Bmp*4 (blue dots). As these cells make contact with each other (b), the secreted *Shh* (red arrow) activates *ptc* on mesenchymal cells and locally downregulates *Fgf*10 (loss of green dots) and upregulates *Bmp*4 (blue dots) expression. The focal downregulation of *Fgf*10 results in lateral subdomains of higher *Fgf*10 expression adjacent to the *Shh* foci that in turn downregulates *Bmp*4, upregulates epithelial *Bmp*7 (yellow arrow), and activates (green arrow) higher epithelial proliferation via epithelial *Fgf*R2*iii*b. The disparate epithelial proliferation rates in the lateral domains result in the sprouting of two buds on each side of the *Shh* foci (blue arrows) that initiates a branch point (d). Further, the elevated *Fgf*10 in the lateral domains upregulates *Shh* and *ptc* expression (d), which allows repetition of the above steps and results in complex branching patterns. The right side of this schematic shows the events following estrogen exposure once bud initiation and ductal elongation (a) are underway. Estradiol directly suppresses mesenchymal *Fgf*10 expression (b) resulting in the inability of cells to form localized morphogen gradients through feedback loops and branching is effectively blocked.

*Bmp*7 in the prostate gland has not been explored, the present findings show that *Bmp*7 is expressed by epithelial cells in the distal signaling center and expression markedly increases during the rapid phase of branching morphogenesis. Moreover, *Fgf*10 upregulates prostatic *Bmp*7 expression, and branching deficits following estrogen exposure coincide with decreased *Bmp*7 expression. Together, these findings suggest a stimulatory role for epithelial *Bmp*7 in prostatic branching with direct positive regulation from mesenchymal *Fgf*10. In contrast, *Fgf*10 downregulates expression of *Bmp*4, an established restrictor of growth and branching in the prostate gland (Lamm et al., 2001). Since *Fgf*10 and *Bmp*4 have opposing actions with regards to prostatic ductal outgrowth, localized downregulation of *Bmp*4 expression by *Fgf*10 may contribute to *Fgf*10's stimulatory effects. Furthermore, since *Shh* upregulates mesenchymal *Bmp*4 expression at focal sites in prostatic ductal tips (Pu et al., 2004), downregulation by *Fgf*10 will contribute to the reciprocal regulation necessary to sculpture the prostatic form (Fig. 12A). Since *Fgf*R2*iii*b is not present on mesenchymal cells, *Bmp*4 downregulation by *Fgf*10 may be mediated through an intermediary signal cascade. Alternatively, *Fgf*10 can ligand to *Fgf*R1*iii*b, a receptor typically expressed in stromal cells, although little is known of its localization and expression in the normal prostate (Foster et al., 1999).

Taken together, we propose that gene regulatory networks organize normal prostate development through a temporal series of reciprocal signals and feedback loops that tightly regulate proliferation, ductal outgrowth, and branch point formation. A simplified working model for prostate branching that incorporates morphoregulatory factors examined herein and in our previous study (Pu et al., 2004) is shown in Fig. 12B (left), although it must be emphasized that several other factors, some characterized, others yet undefined, will undoubtedly play critical roles in this process. As prostatic buds emerge from the UGS (a), they grow toward the distal mesenchyme, perhaps in response to chemoattraction by *Fgf*10. The epithelial cells at the distal signaling center express *Shh*, highly localized in discreet foci (Pu et al., 2004), as well as *Bmp*7, whereas the distal mesenchyme expresses *Fgf*10 and *Bmp*4. When *Shh* foci in the elongating ducts make contact with the *Fgf*10 and *Bmp*4-expressing cells (b), *Fgf*10 is focally downregulated and *Bmp*4 is focally upregulated by *Shh* as previously described (Pu et al., 2004), which leads to lateral subdomains of elevated *Fgf*10 expression. Within those lateral subdomains, relatively higher *Fgf*10 levels downregulate mesenchymal *Bmp*4 expression and thus release the *Bmp*4 brake on ductal outgrowth. At the lateral domains, *Fgf*10 directly increases epithelial *Bmp*7 expression and epithelial cell proliferation via epithelial *Fgf*R2*iii*b (c). The disparate epithelial proliferation rates at these lateral domains result in the sprouting of two buds thus initiating a branch point (c). *Fgf*10 at the branching tips increases epithelial *Shh* (d), which allows the process to repeat itself thus resulting in complex branching patterns characteristic of the prostate gland. In this manner, epithelial–mesenchymal cross-talk via secreted morphogens and their tightly controlled feedback loops maintain controlled branching morphogenesis. Importantly, interruption of this signaling network by altered expression of *Fgf*10, *Shh*, *Bmp*4, and *Bmp*7 or their cognate receptors will result in growth and branching abnormalities.

Suppression of Fgf10 signaling mediates the estrogenized branching phenotype in the dorsolateral prostate

We previously demonstrated that LP and DP, but not VP, have severe branching deficits following neonatal estrogen exposure and that this is related to a lobe-specific suppression of *Shh-ptc-gli* in the DLP (Pu et al., 2004). However, ERα, which initiates the cascade of events following estrogen exposure, is expressed in prostatic mesenchymal cells (Prins and Birch, 1997; Prins et al., 2001a,b), which suggests an intermediary pathway in this process. The present findings provide several lines of evidence to implicate *Fgf*10 as a critical mesenchymal signal that mediates estrogen-induced branching inhibition in the DLP. First, *Fgf*10 is expressed in the same population of periductal mesenchymal cells where ERα is upregulated following estrogen exposure (Prins and Birch, 1997), thus direct regulation is possible. Second, *Fgf*R2*iii*b is expressed in the distal epithelium and *Fgf*10 upregulates prostatic *Shh* and *Bmp*7 expression in those same cells. Third, a parallel suppression of *Fgf*10, *Shh-ptc-gli*, and *Bmp*7 is observed specifically in the LP following estradiol exposure while VP expression of these signaling molecules is unaffected. Fourth, as demonstrated by organ culture, estradiol suppression of *Fgf*10 and *Fgf*R2*iii*b us mediated directly at the prostatic level. Fifth, and most importantly, *Fgf*10 replacement rescues the growth and differentiation suppression induced by estradiol in the LP. This contrasts with the inability of *Shh* beads to reverse estrogen-induced growth inhibition (unpublished data) and the ability of *Bmp*4 antagonists to only partially reverse estrogen effects (Huang et al., 2003). Taken together with the above data that *Fgf*10 is a regulator of prostatic *Shh*, *Bmp*4, and *Bmp*7 expression, these findings suggest that *Fgf*10 suppression may be a proximate cause of the branching phenotype in the LP following neonatal estrogen exposure. This phenomenon is graphically represented in Fig. 12B (right).

In the normal developing prostate, ERα expression is restricted to proximal mesenchymal cells where it may be involved in maintaining a proximal structure by suppressing proximal expression of *Fgf*10 and other genes expressed in the distal prostate. When rats are exposed neonatally to estrogen, ERα expression is induced in periductal mesenchymal cells along the ductal length out to the distal tips in all lobes (Prins and Birch, 1997). We propose that this may downregulate *Fgf*10 and other morphoregulatory genes in the distal signaling center, thus resulting in the proximalized phenotype previously charac-

terized by our laboratory (Prins et al., 2001a,b). It is also possible that altered retinoid signaling contributes to reduced *Fgf*10 expression as it does in the lung (Cardoso, 2001). This is notable since we have observed DLP-specific expression of retinoid metabolizing enzymes and binding proteins during prostatic development as well as lobe-specific alterations in retinoid receptors, binding proteins, and metabolizing enzymes following neonatal estrogen exposure (Prins et al., 2002; Pu et al., 2003). Thus, lobe-specific alterations in *Fgf*10 signaling could be a result of estrogen-induced, lobe-specific alterations in retinoid signaling. Recently, *Tgf*β1 was shown to down-regulate prostatic *Fgf*10 expression (Tomlinson et al., 2004), and this pathway may also be involved in the estrogen-induced downregulation of *Fgf*10 since we have previously observed an increase in latent and active *Tgf*β1 in stromal cells following neonatal estrogen exposure (Chang et al., 1999). Perhaps multiple pathways contribute to the alterations in expression of *Fgf*10 and other genes following estrogen exposure that leads to the lobe-specific and complex estrogenized phenotype. It is important to note that since *Fgf*10 does not autoregulate *Fgf*R2*iii*b, the estrogen effect of decreased epithelial *Fgf*R2 is most likely not directly mediated through *Fgf*10 downregulation and may involve these other pathways.

In conclusion, the present study provides evidence for regulatory gene networks during prostate development that allows for localized morphoregulatory factor expression and controlled branching morphogenesis. Induction of positive and negative regulators to modulate signaling activity is a recurring theme in developing branched structures (Chuang and McMahon, 2003), and the present findings demonstrate that this process applies to the prostate gland as well. Our findings also show that the lobe-specific responses to neonatal estrogen exposures are a result of lobe-specific alterations in the expression of several of these secreted morphogens and their cognate receptors. Downregulation of *Fgf*10 signaling appears to be a proximate cause of the altered signaling cascade leading to branching deficits in the dorsolateral prostate gland.

Acknowledgments

The authors gratefully thank Dr. Oliver Putz for graphic renditions of our data. The work was supported by NIH grant DK-40890.

References

Aboseif, S.R., Dahiya, R., Narayan, P., Cunha, G.R., 1997. Effect of retinoic acid on prostatic development. Prostate 31, 161–167.

Bellusci, S., Grindley, J., Emoto, H., Itoh, N., Hogan, B., 1997. Fibroblast growth factor 10 (FGF10) and branching morphogenesis in the embryonic mouse lung. Development 124, 4867–4878.

Bhatia-Gaur, R., Donjacour, A.A., Sciavolino, P.J., Kim, M., Desai, N., Young, P., Norton, C.R., Gridley, T., Cardiff, R.D., Cunha, G.R., Abate-Shen, C., Shen, M.M., 1999. Roles for Nkx3.1 in prostate development and cancer. Genes Dev. 13, 966–977.

Cardoso, W.V., 2000. Lung morphogenesis revisited: old facts, current ideas. Dev. Dyn. 219, 121–130.

Cardoso, W.V., 2001. Molecular regulation of lung development. Annu. Rev. Physiol. 63, 471–494.

Chang, W.Y., Birch, L., Woodham, C., Gold, L.I., Prins, G.S., 1999. Neonatal estrogen exposure alters the transforming growth factor-β signaling system in the developing rat prostate and blocks the transient $p21^{cip1/wafl}$ expression associated with epithelial differentiation. Endocrinology 140, 2801–2813.

Chuang, P.-T., McMahon, A.P., 2003. Branching morphogenesis of the lung: new molecular insights into an old problem. Trends Cell Biol. 13, 86–91.

Desai, T.J., Mapel, S., Flentke, G.R., Smith, S.M., Cardoso, W.V., 2004. Retinoic acid selectively regulates Fgf10 expression and maintains cell identity in the prospective lung field of the developing foregut. Dev. Biol. 273, 402–415.

Donjacour, A.A., Thomson, A.A., Cunha, G., 2003. FGF-10 plays an essential role in the growth of the fetal prostate. Dev. Biol. 261, 39–54.

Economides, K.D., Capecchi, M.R., 2003. *Hoxb13* is required for normal differentiation and secretory function of the ventral prostate. Development 130, 2061–2069.

Finch, P., Cunha, G., Rubin, J., Wong, J., Ron, D., 1995. Pattern of keratinocyte growth factor and keratinocyte growth factor receptor expression during mouse fetal development suggests a role in mediating morphogenetic mesenchymal–epithelial interactions. Dev. Dyn. 203, 223–240.

Foster, B., Kaplan, P., Greenberg, N., 1999. Characterization of the FGF axis and identification of a novel FGFR1iic isoform during prostate cancer progression in the TRAMP model. Prostate Cancer Prospatic Dis. 2, 76–82.

Gilleran, J.P., Putz, O., De Jong, M., De Jong, S., Birch, L., Pu, Y., Huang, L., Prins, G.S., 2003. The role of prolactin in the prostatic inflammatory response to neonatal estrogen. Endocrinology 144, 2046–2054.

Habermann, H., Chang, W.Y., Birch, L., Parmender, M., Prins, G.S., 2001. Developmental exposure to estrogens alters epithelial cell adhesion and gap junction proteins in the adult rat prostate. Endocrinology 142, 359–369.

Haraguchi, R., Suzuki, K., Murakami, R., Sakai, M., Kamikawa, M., Kengaku, M., Sekine, K., Kawano, H., Kato, S., Ueno, N., Yamada, G., 2000. Molecular analysis of external genitalia formation: the role of fibroblast growth factor (Fgf) genes during genital tubercle formation. Development 127, 2471–2479.

Hayashi, N., Sugimura, Y., Kawamura, J., Donjacour, A.A., Cunha, G.R., 1991. Morphological and functional heterogeneity in the rat prostatic gland. Biol. Reprod. 45, 308–321.

Hoffman, M.P., Kidder, B.L., Steinberg, Z.L., Lakhani, S., Ho, S.M., Kleinman, H.K., Laresen, M., 2002. Gene expression profiles of mouse submandibular gland development: FGFR1 regulates branching morphogenesis in vitro through BMP- and FGF-dependent mechanisms. Development 129, 5767–5778.

Huang, L., Pu, Y., Alam, S., Prins, G.S., 2003. Neonatal estrogen exposure disrupts prostate morphogenesis through alterations in BMP-4, BMP-7 and FGF-10 expression. The Endocrine Society's 85th Annual Meeting. Philadelphia, PA, the Endocrine Society, Bethesda, MD, p. 334. Abstract # P332-113.

Huang, L., Pu, Y., Alam, S., Birch, L., Prins, G.S., 2004. Estrogenic regulation of signaling pathways and homeobox genes during rat prostate development. J. Androl. 25, 330–337.

Lamm, M.L., Podlasek, C.A., Barnett, D.H., Lee, J., Clemens, J.Q., Hebner, C.M., Bushman, W., 2001. Mesenchymal factor bone morphogenetic protein 4 restricts ductal budding and branching morphogenesis in the developing prostate. Dev. Biol. 232, 301–314.

Lamm, M.L., Catbagan, W.S., Laciak, R.J., Barnett, D.H., Hebner, C.M., Gaffield, W., Walterhouse, D., Iannaccone, P., Bushman, W., 2002. Sonic hedgehog activates mesenchymal Gli1 expression during prostate ductal bud formation. Dev. Biol. 249, 349–366.

Lu, W., Luo, Y., Kan, M., McKeehan, W.L., 1999. Fibroblast growth factor-10: a second candidate stromal to epithelial cell andromedin in prostate. J. Biol. Chem. 274, 12827–12834.

McGinley, J.N., Knott, K.K., Thompson, H.J., 2000. Effect of fixation and epitope retrival on BrdU indices in mammary carcinomas. J. Histochem. Cytochem. 48, 355–362.

Ohuchi, H., Nakagawa, T., Yamamoto, A., Araga, A., Ohata, T., Ishimaru, Y., Yoshioka, H., Kuwana, T., Nohno, T., Yamasaki, M., Itoh, N., Noji, S., 1997. The mesenchymal factor, FGF10, initiates and maintains the outgrowth of the chick limb bud through interaction with FGF8, an apical ectodermal factor. Development 124, 2235–2244.

Ornitz, D.M., Itoh, N., 2001. Fibroblast growth factors. Genome Biol. 2, 1–12.

Peters, K., Werner, S., Liao, X., Wert, S., Whitsett, J., Williams, L., 1994. Targeted expression of a dominant negative FGF receptor blocks branching morphogenesis and epithelial differentiation of the mouse lung. EMBO J. 13, 3296–3301.

Price, D., 1936. Normal development of the prostate and seminal vesicles of the rat with a study of experimental postnatal modifications. Am. J. Anat. 60, 79–127.

Prins, G.S., 1992. Neonatal estrogen exposure induces lobe-specific alterations in adult rat prostate androgen receptor expression. Endocrinology 130, 3703–3714.

Prins, G.S., 1997. Developmental estrogenization of the prostate gland. In: Naz, R.K. (Ed.), Prostate: Basic and Clinical Aspects. C.R.C. Press, Boca Raton, p. 247–265. Chap. 10.

Prins, G.S., Birch, L., 1995. The developmental pattern of androgen receptor expression in rat prostate lobes is altered after neonatal exposure to estrogen. Endocrinology 136, 1303–1314.

Prins, G.S., Birch, L., 1997. Neonatal estrogen exposure up-regulates estrogen receptor expression in the developing and adult rat prostate lobes. Endocrinology 138, 1801–1809.

Prins, G.S., Birch, L., Greene, G.L., 1991. Androgen receptor localization in different cell types of the adult rat prostate. Endocrinology 129, 3187–3199.

Prins, G.S., Woodham, C., Lepinske, M., Birch, L., 1993. Effects of neonatal estrogen exposure on prostatic secretory genes and their correlation with androgen receptor expression in the separate prostate lobes of the adult rat. Endocrinology 132, 2387–2398.

Prins, G.S., Birch, L., Couse, J.F., Choi, I., Katzenellenbogen, B., Korach, K.S., 2001a. Estrogen imprinting of the developing prostate gland in mediated through stromal estrogen receptor α: studies with αERKO and βERKO mice. Cancer Res. 61, 6089–6097.

Prins, G.S., Birch, L., Habermann, H., Chang, W.Y., Tebeau, C., Putz, O., Bieberich, C., 2001b. Influence of neonatal estrogens on rat prostate development. Reprod. Fertil. Dev. 13, 241–252.

Prins, G.S., Chang, W.Y., Wang, Y., van Breemen, R.B., 2002. Retinoic acid receptors and retinoids are up-regulated in the developing and adult rat prostate by neonatal estrogen exposure. Endocrinology 143, 3628–3640.

Pu, Y., Deng, L., Davies, P.J.P., Prins, G.S., 2003. Retinoic acid metabolizing enzymes, binding proteins and RXRs are differentially expressed in the developing and adult rat prostate lobes and are altered by neonatal estrogens in a lobe-specific manner. The Endocrine Society's 85th Annual Meeting, Philadelphia, PA, the Endocrine Society, Bethesda, MD, p. 530. Abstract # P533-236.

Pu, Y., Huang, L., Prins, G.S., 2004. Sonic hedgehog-patched-Gli signaling in the developing rat prostate gland: lobe-specific suppression by neonatal estrogens reduces ductal growth and branching. Dev. Biol. 273, 257–275.

Putz, O., Prins, G.S., 2002. Prostate gland development and estrogenic imprinting. In: Burnstein, K.L. (Ed.), Steroid Hormones and Cell Cycle Regulation. Kluwer Academic Publishers, Boston, MA, p. 73–89.

Putz, O., Schwartz, C.B., Kim, S., LeBlanc, G.A., Cooper, R.L., Prins, G.S., 2001. Neonatal low- and high-dose exposure to estradiol benzoate in the male rat: I. Effects on the prostate gland. Biol. Reprod. 65, 1496–1505.

Raman, R., Venkataraman, G., Ernst, S., Sasisekharan, V., Sasisekharan, R., 2003. Structural specificity of heparin binding growth factor family of proteins. Proc. Natl. Acad. Sci. 100, 2357–2362.

Revest, J.-M., Spencer-Dene, B., Kerr, K., De Moerlooze, L., Rosewell, I., Dickson, C., 2001. Fibroblast growth factor receptor 2-IIIb acts upstream of *Shh* and *Fgf4* and is required for limb bud maintenance but not for the induction of *Fgf8*, *Fgf10*, *Msx1*, or *Bmp4*. Dev. Biol. 231, 47–62.

Robertson, F.G., Harris, J., Naylor, M.J., Oakes, S.R., Kindblom, J., LDillner, K., Wennbo, H., Tornell, J., Kelly, P.A., Green, J., Ormandy, C.J., 2003. Prostate development and carcinogenesis in prolactin receptor knockout mice. Endocrinology 144, 3196–3205.

Ruan, W., Powell-Braxton, L., Kopchick, J.J., Kleinberg, D.L., 1999. Evidence that insulin-like growth factor I and growth hormone are required for prostate gland development. Endocrinology 140, 1984–1989.

Sabharwal, V., Putz, O., Prins, G.S., 2000. Neonatal estrogen exposure induces progesterone receptor expression in the developing prostate gland. 95th Annual Meeting of the American Urologic Association. Atlanta, GA, the Endocrine Society, Bethesda, MD, p. 97.

Seo, R., McGuire, M., Chung, M., Bushman, W., 1997. Inhibition of prostate ductal morphogenesis by retinoic acid. J. Urol. 158, 931–935.

Szebenyi, G., Fallon, J.F., 1999. Fibroblast growth factors as multifunctional signaling factors. Int. Rev. Cyt. 185, 45–106.

Thomson, A.A., Cunha, G.R., 1999. Prostatic growth and development are regulated by FGF10. Development 126, 3693–3701.

Tomlinson, D.C., Gindley, J.C., Thomson, A.A., 2004. Regulation of Fgf10 gene expression in the prostate: identification of transforming growth factor-β1 and promoter elements. Endocrinology 145, 1988–1995.

Uematsu, F., Kan, M., Wang, F., Jang, J.H., Luo, Y., McKeehan, W.L., 2000. Ligand binding properties of binary complexes of heparin and immunoglobulin-like modules of FGF receptor 2. Biochem. Biophys. Res. Commun. 272, 830–836.

Weaver, M., Dunn, N.R., Hogan, B.L., 2000. BMP4 and FGF10 play opposing roles during lung bud morphogenesis. Development 127, 2695–2704.

Woodham, C., Birch, L., Prins, G.S., 2003. Neonatal estrogens down regulate prostatic androgen receptor levels through a proteosome-mediated protein degradation pathway. Endocrinology 144, 4841–4850.